

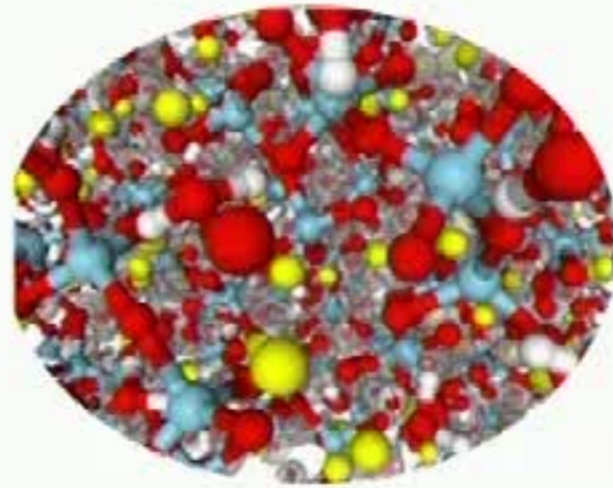
Materials discovery and scientific design by computation: what does it take?

Giulia Galli

University of Chicago
& Argonne National Laboratory

2018 SIAM Annual Meeting, Portland, July 13th, 2018

Materials: solids, liquids, nanostructures and combinations thereof



Materials: solids, liquids, nanostructures and combinations thereof

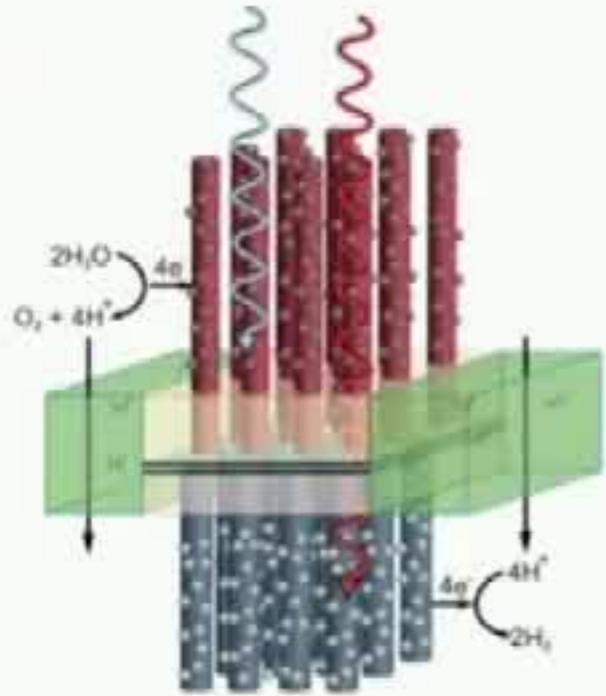
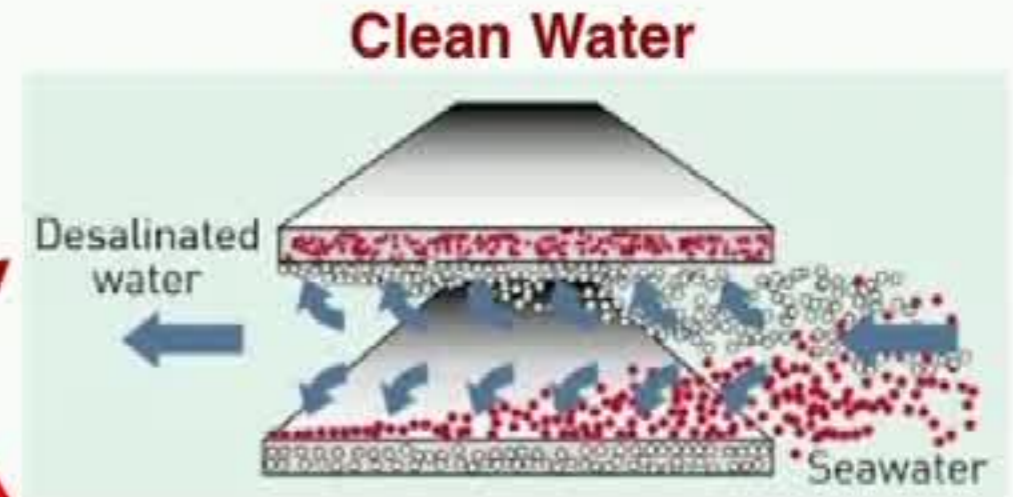


Photo-electrochemical cells



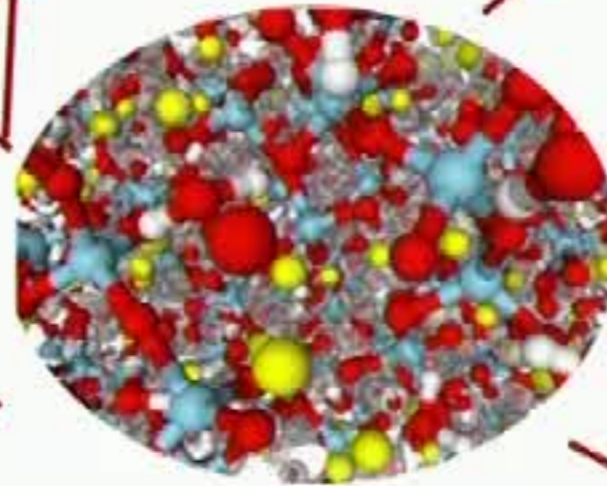
Solar cells



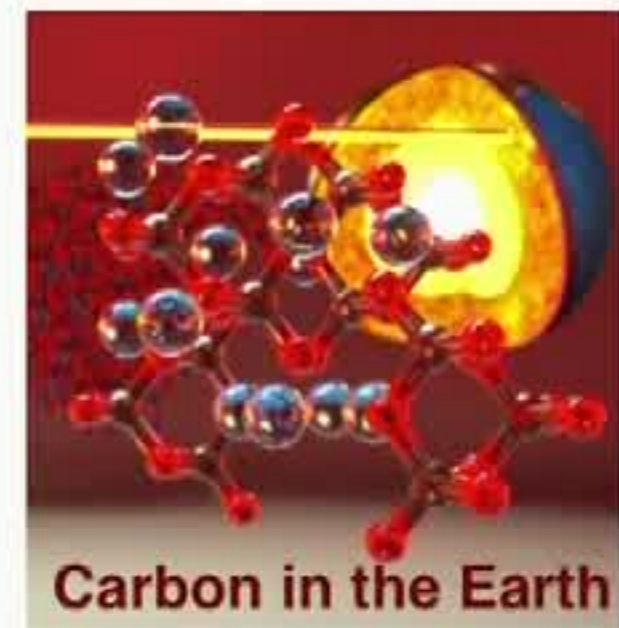
Clean Water

Desalinated water

Seawater

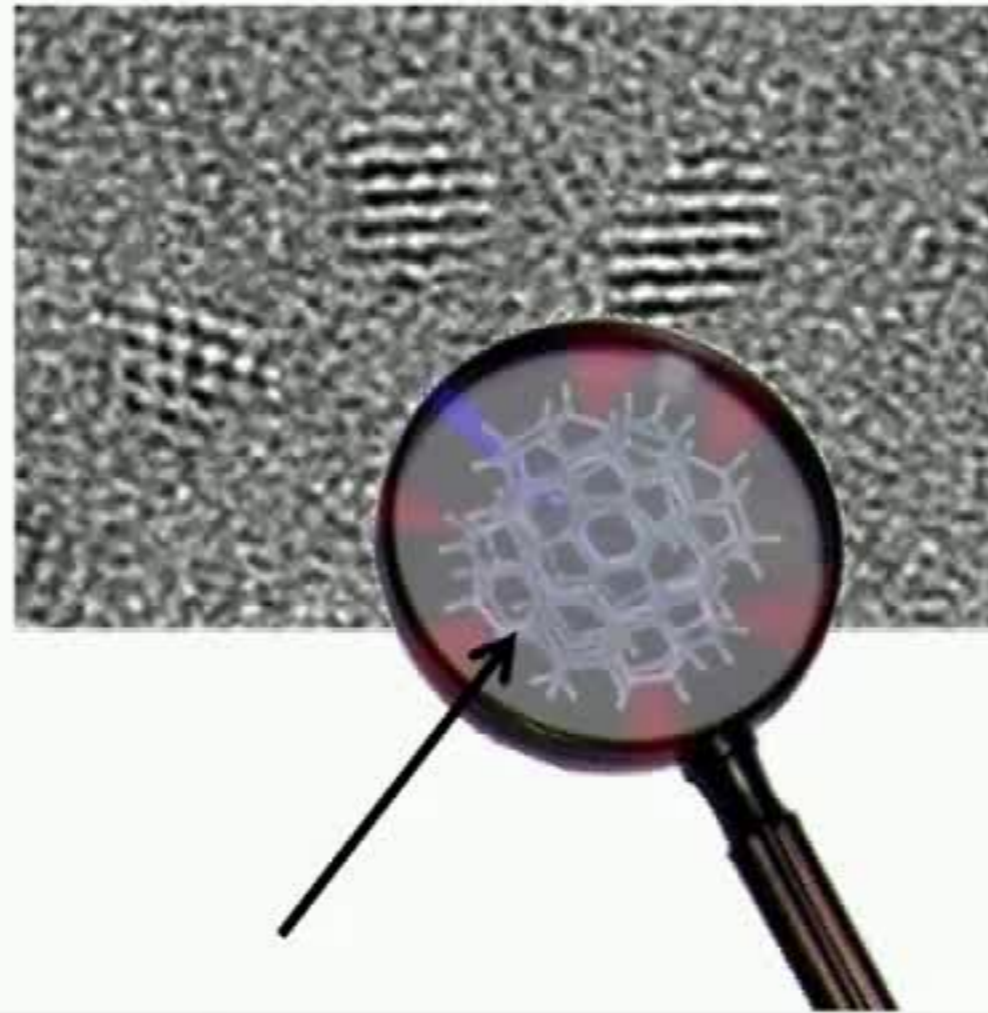


Qubits



Carbon in the Earth

At the microscopic scale



Nuclei: $\{R_I\}_I$
Electrons: $\{\psi_i\}_i$

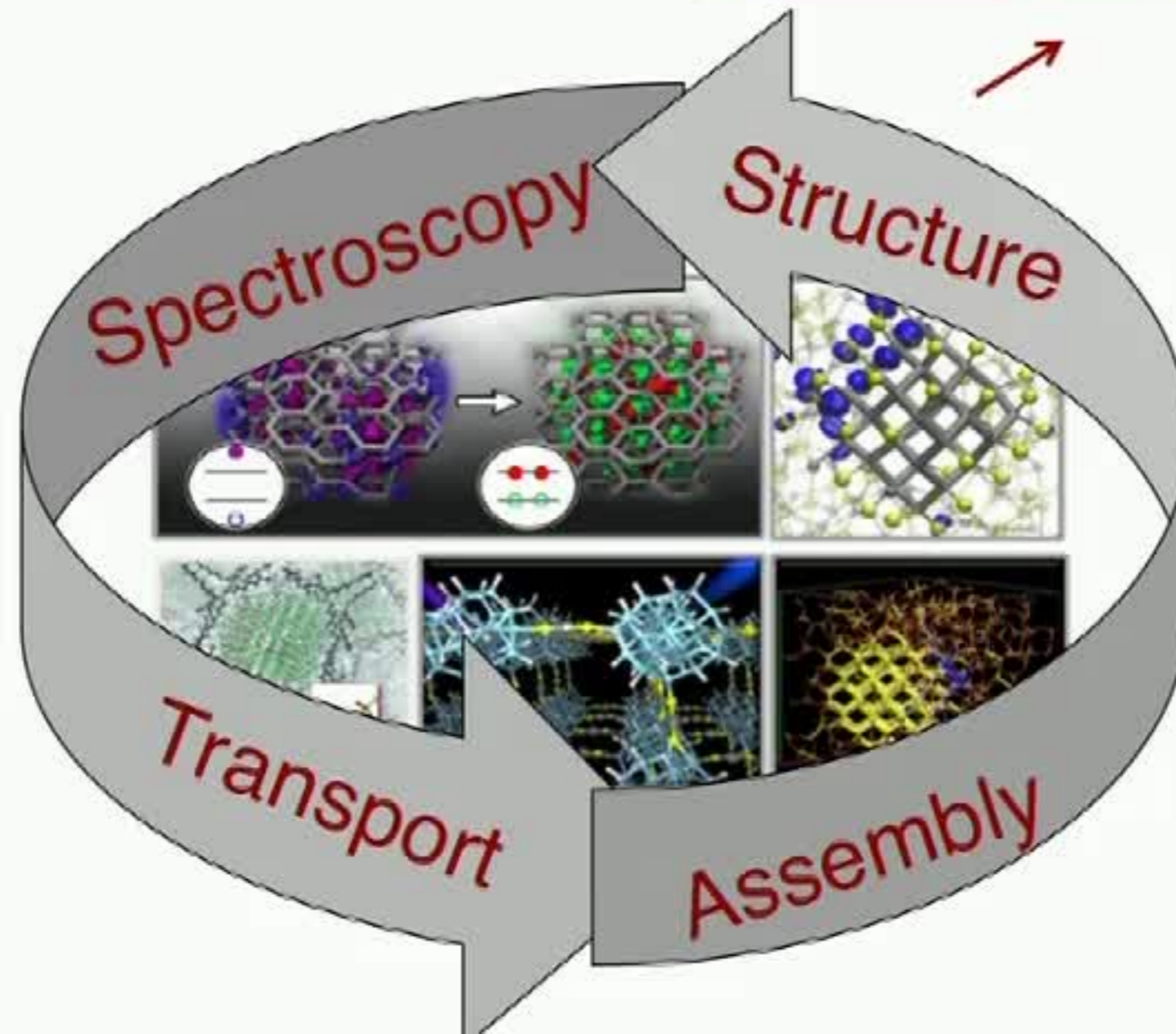
Materials are complex systems

- Realistic materials are **heterogeneous systems**
 - Understand and control the role of interfaces and defects
- Discovery and design of materials and emergent behaviors require the ability to compute **multiple properties**
 - Simulations at different length and time scales
- Desired & new functionalities of materials may arise from assembling **building blocks**
 - Design building blocks with targeted properties and assemble them with precision
- Desired & new functionalities may arise in **metastable systems**
 - Investigate out of equilibrium processes
 - Simulate assembly processes during synthesis

Integrated predictions of multiple properties

Integrated predictions of multiple properties

Geometrical arrangements of atoms; thermodynamic properties from approximate solutions of the **Schroedinger equation**



Quantum mechanics: approximations and computation

The approximations:

- Mean-field theories: $E_0(\{\mathbf{R}_I\}) = \text{Min}_{n(\mathbf{r})} E_{\{\mathbf{R}\}}[n]$

- Density Functional Theory

- *Local density approximations*

- Hartree-Fock and Quantum Chemistry

- Stochastic approaches:

- Quantum Monte Carlo

- *The fixed node approximation*

~ 1965

~ 1985-1990

~ 1980

Quantum mechanics: approximations and computation

The approximations:

- Mean-field theories: $E_0(\{\mathbf{R}_I\}) = \text{Min}_{n(\mathbf{r})} E_{\{\mathbf{R}\}}[n]$

- Density Functional Theory

- *Local density approximations*

- Hartree-Fock and Quantum Chemistry

- Stochastic approaches:

- Quantum Monte Carlo

- *The fixed node approximation*

~ 1965

~ 1985-1990

~ 1980

The ability to compute:

In the 1990s, Density Functional theory and quantum chemistry are massively used in physics and chemistry, as the results of key **algorithmic and computational developments**. Quantum Monte Carlo is applied to “real materials”.

Quantum mechanics: approximations and computation

The approximations:

- Mean-field theories: $E_0(\{\mathbf{R}_I\}) = \text{Min}_{n(\mathbf{r})} E_{\{\mathbf{R}\}}[n]$

- Density Functional Theory (DFT)

- *Local density approximations*

- Hartree-Fock and Quantum Chemistry

- Stochastic approaches:

- Quantum Monte Carlo (QMC)

- *The fixed node approximation*

~ 1965

~ 1985-1990

~ 1980

Molecular Dynamics
(MD) with forces from
DFT → *ab-initio MD*:

**Dynamical and
thermodynamic
properties from first
principles**

The ability to compute:

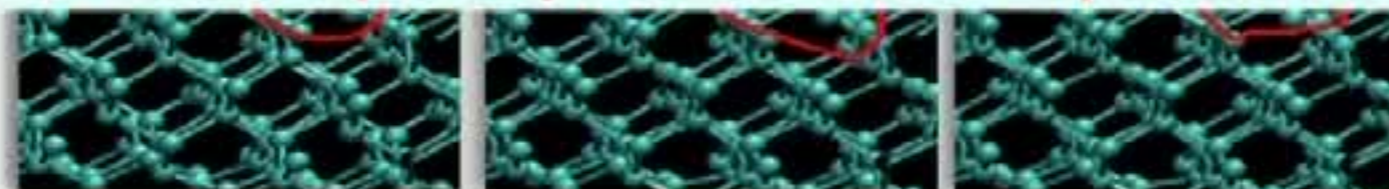
algorithmic and computational developments

- All-electron solutions to DFT equations
- *Ab-initio* Molecular Dynamics (Car-Parrinello method)
- Linear scaling methods within DFT and QMC
- Software development for HPC architectures

Ab initio Molecular Dynamics



From first principles: no fit to experiments



$$M_i \ddot{R}_i = F_i$$
$$F_i = -\nabla_i \mathbf{E}(\{R_i(t)\})$$



\mathbf{E} from Density Functional Theory



Solve set of N coupled, non linear partial differential equations self-consistently, using iterative algorithms, subject to orthonormality constraints. $N = \#$ of electrons

Complexity of *ab initio* MD: Kohn Sham equations

Solve set of **N** coupled, non linear partial differential equations self-consistently, using iterative algorithms, subject to orthonormality constraints. **N** = # of electrons

Condensed Matter Physics



Physical Chemistry

$$-\Delta\varphi_i + V(\rho, \mathbf{r})\varphi_i = \varepsilon_i\varphi_i \quad i = 1 \dots N_{\text{el}}$$

$$V(\rho, \mathbf{r}) = V_{\text{ion}}(\mathbf{r}) + \int \frac{\rho(\mathbf{r}')}{|\mathbf{r} - \mathbf{r}'|} d\mathbf{r}' + V_{\text{XC}}(\rho(\mathbf{r}), \nabla\rho(\mathbf{r}))$$

Hybrid Functionals (*)

$$\rho(\mathbf{r}) = \sum_{i=1}^{N_{\text{el}}} |\varphi_i(\mathbf{r})|^2$$



$$\int \varphi_i^*(\mathbf{r}) \varphi_j(\mathbf{r}) d\mathbf{r} = \delta_{ij}$$

The cost of solving the Kohn-Sham equations is eventually dominated by orthogonalization ($O(N^3)$)

Why its finding existing eigensolvers is difficult

- Non linear fix-point problem solved using iterative methods to find self-consistent solutions
- Existing eigensolvers may be used in inner loops (fixed potential), but:
 - Solutions are required at each MD time step (tens of thousands of steps during MD)
- For many systems only the lowest invariant subspace is needed (linear combination of eigenvectors, not starting point of iterative)
- Full procedure of eigenvalues and eigenvalues not needed in early stages
- Number of self-consistent iterations may vary at each MD step
 - Threshold for convergence depends on outer loop (specifically, on large basis sets (millions of basis functions))
- Usually tens of thousands of eigenvectors are needed
- Spectra does not necessarily have a gap and the existence of a gap is not known beforehand
- Cost of matrix-vector product is cubic in the number of electrons

Existing eigensolvers (Scalapack, ELPA) are used to solve the Ritz problem, once the invariant subspace has been determined

Some examples Why using existing eigen solvers is difficult

Existing eigen solvers may be used in inner loops (fixed potential), but:

- PNAS 2018 For many systems only the lowest invariant subspace is needed (linear combinations of eigenvectors, not individual eigenvectors)
- Nature Comm. 2018 Full accuracy of eigenvectors and eigenvalues not needed in early stages of self-consistent iterations
 - Threshold for convergence depends on outer loop (specifically, on the value of a functional of eigenvectors)
- Parallel data layout of existing eigen solvers not always compatible with data layout of other parts of the application, implying substantial data transfer

Existing eigen solvers (Scalapack, ELPA) are used to solve the Ritz problem, once the invariant subspace has been determined

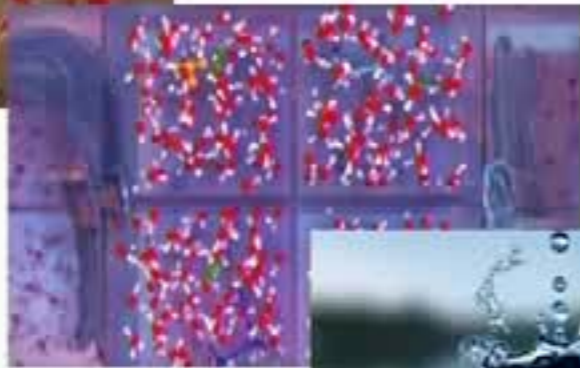
Some examples

Liquids



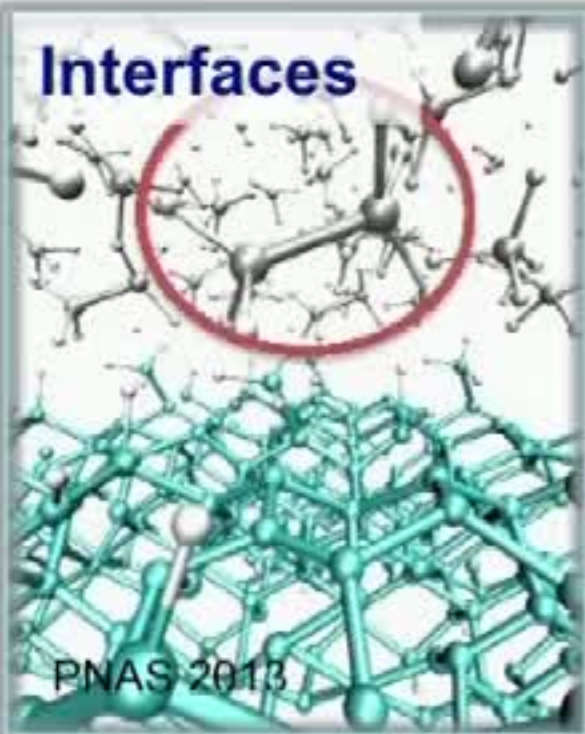
JPC-Lett. 2017

PNAS 2018



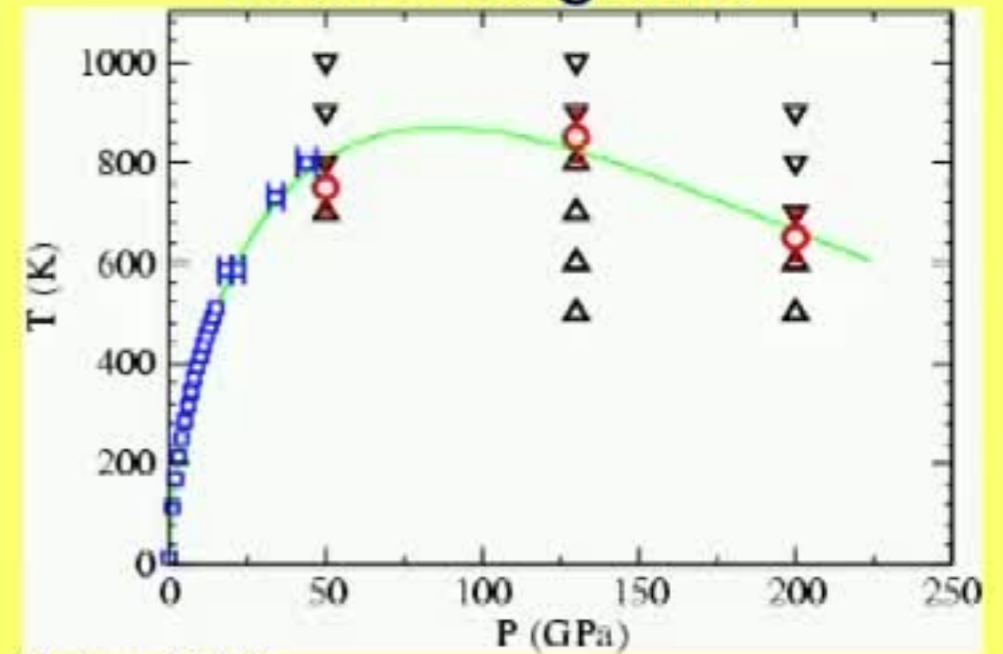
Nature Comm. 2018

Interfaces



PNAS 2013

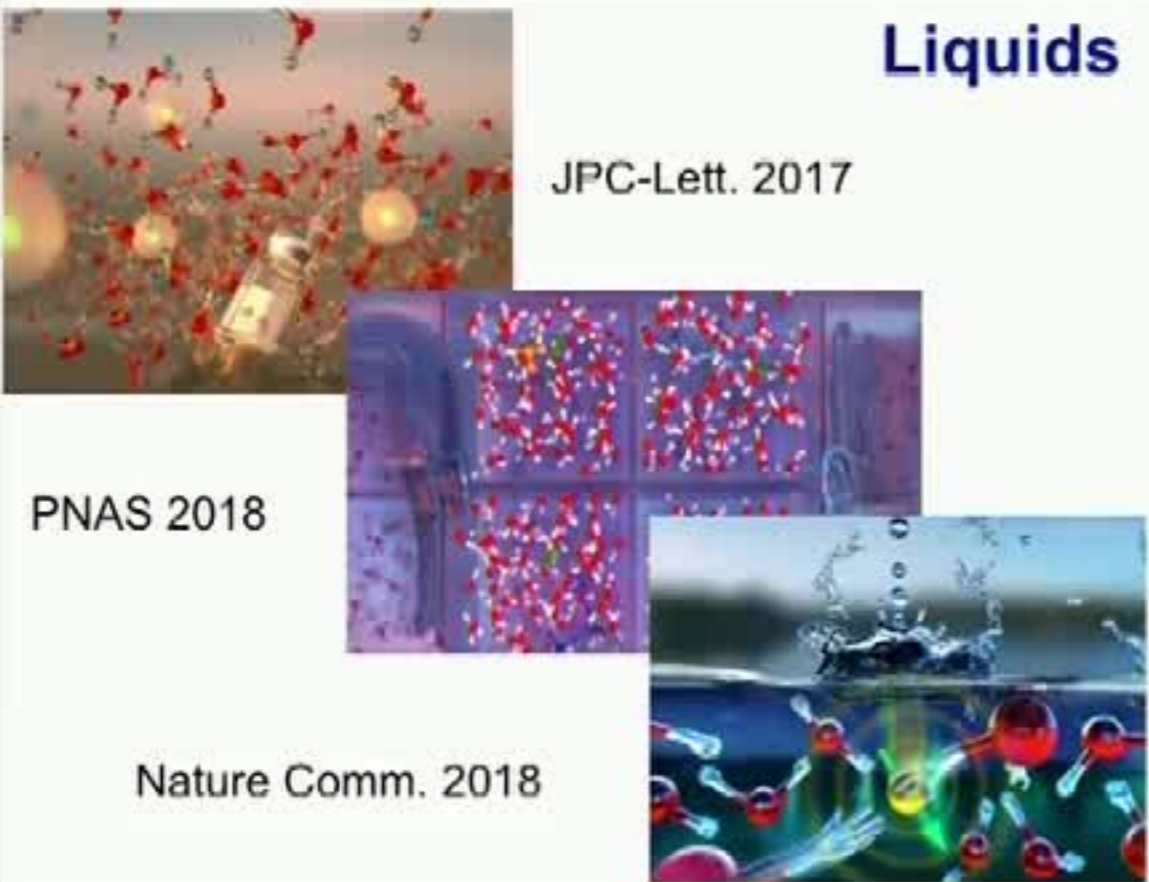
Phase diagrams



Nature 2004

Some examples

Liquids

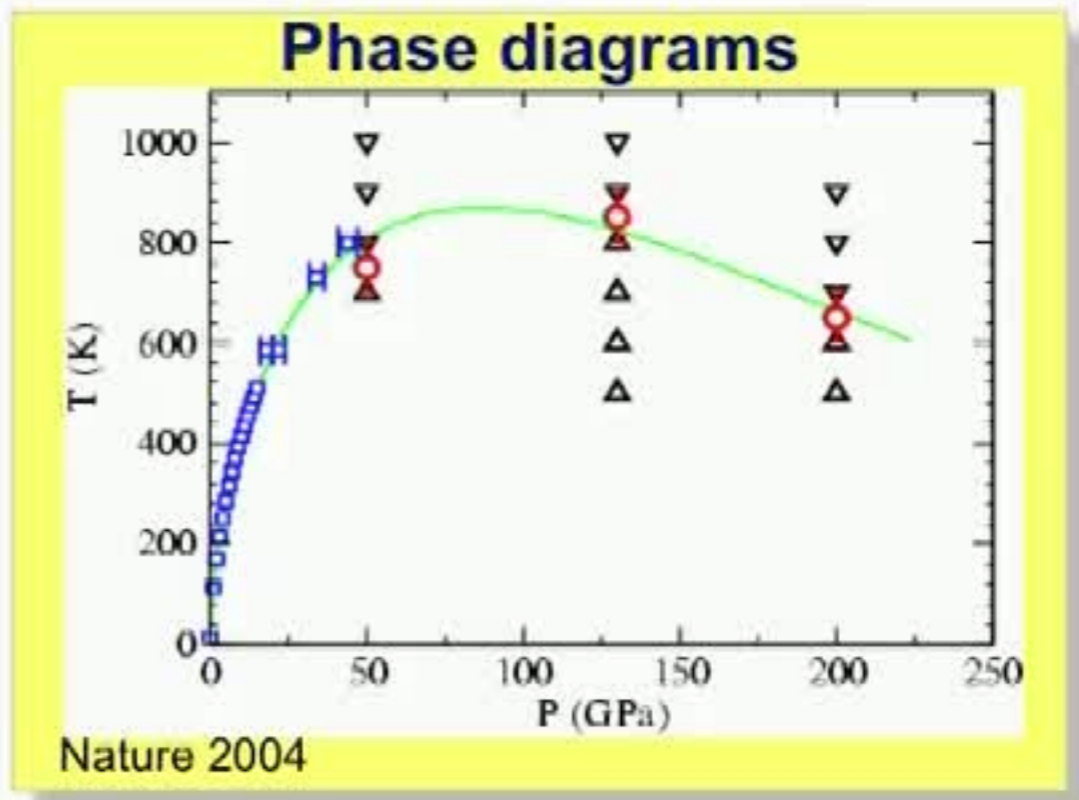


JPC-Lett. 2017

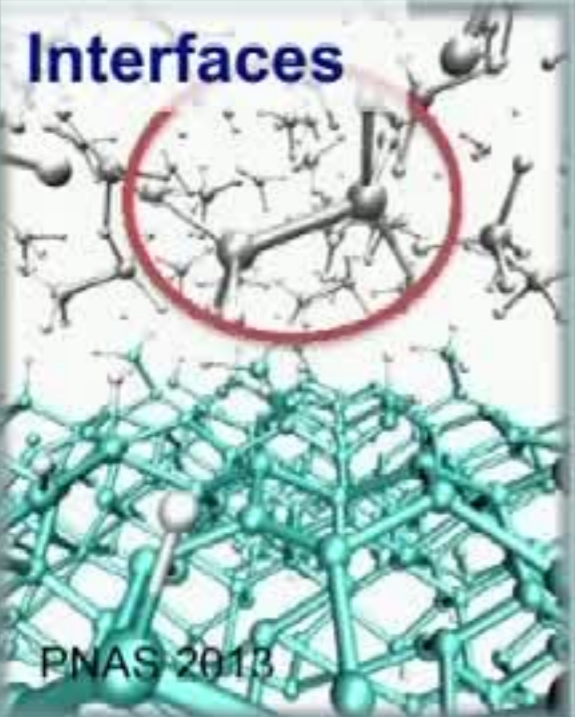
PNAS 2018

Nature Comm. 2018

The image shows a molecular dynamics simulation of a liquid surface. At the top left, a water droplet is shown splashing, with red and white spheres representing oxygen and hydrogen atoms respectively. Below this, there are several panels showing the molecular structure of the liquid surface, with a focus on the hydrogen bonding network. The bottom right panel shows a close-up of the water molecules at the surface, with a green and blue glow highlighting specific interactions.



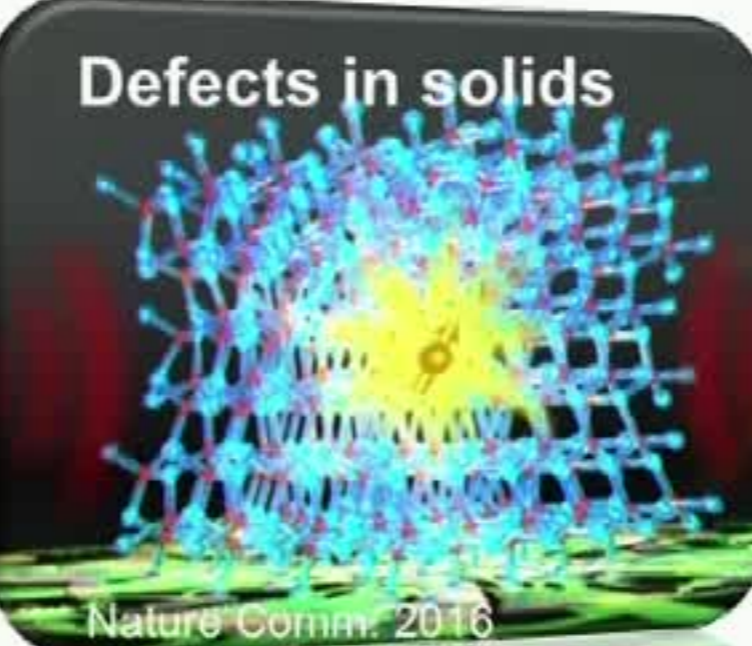
Interfaces



PNAS 2013

The image shows a molecular dynamics simulation of a solid-liquid interface. The top part shows a disordered network of atoms, while the bottom part shows a more ordered, crystalline structure. A red circle highlights a specific region at the interface where the structure is changing.

Defects in solids

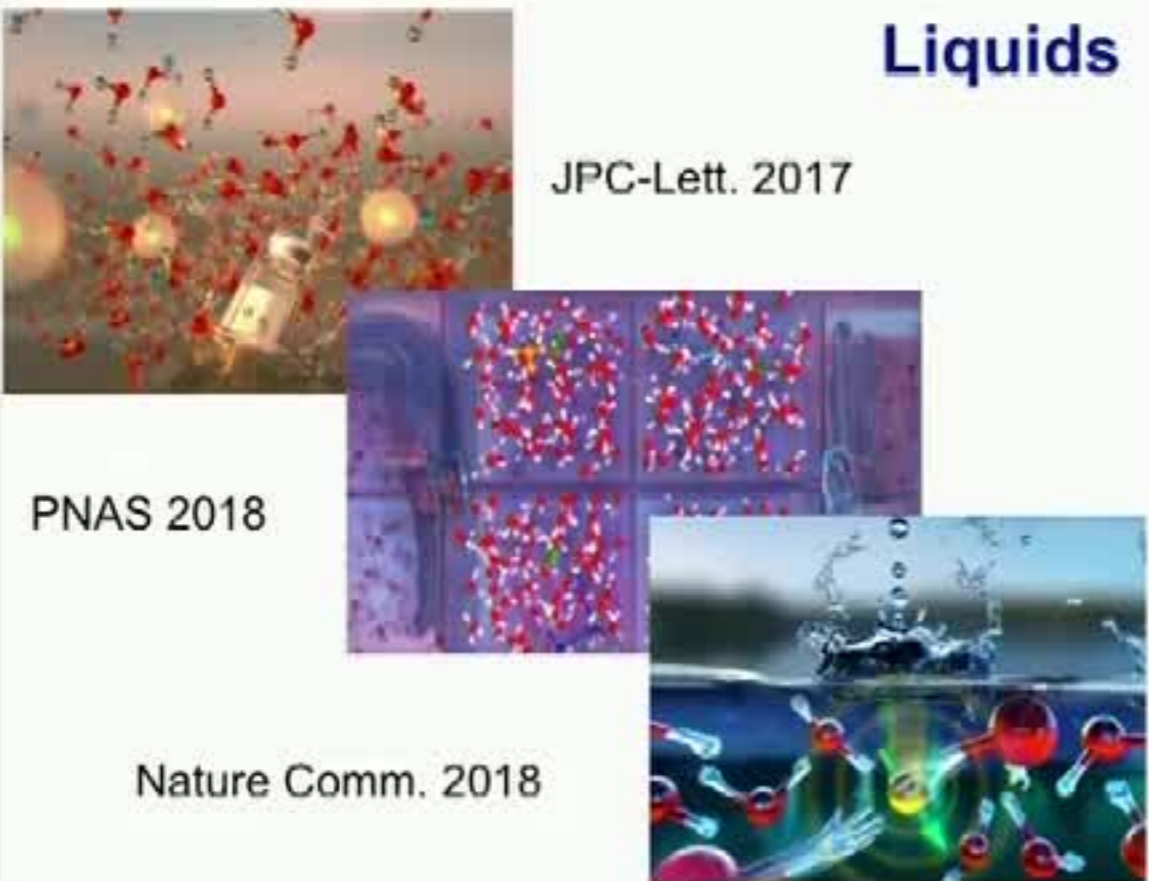


Nature Comm. 2016

The image shows a molecular dynamics simulation of a defect in a solid lattice. The atoms are represented by blue and red spheres. A central region is highlighted in yellow, indicating a defect or a specific site of interest within the crystal structure.

Some examples

Liquids

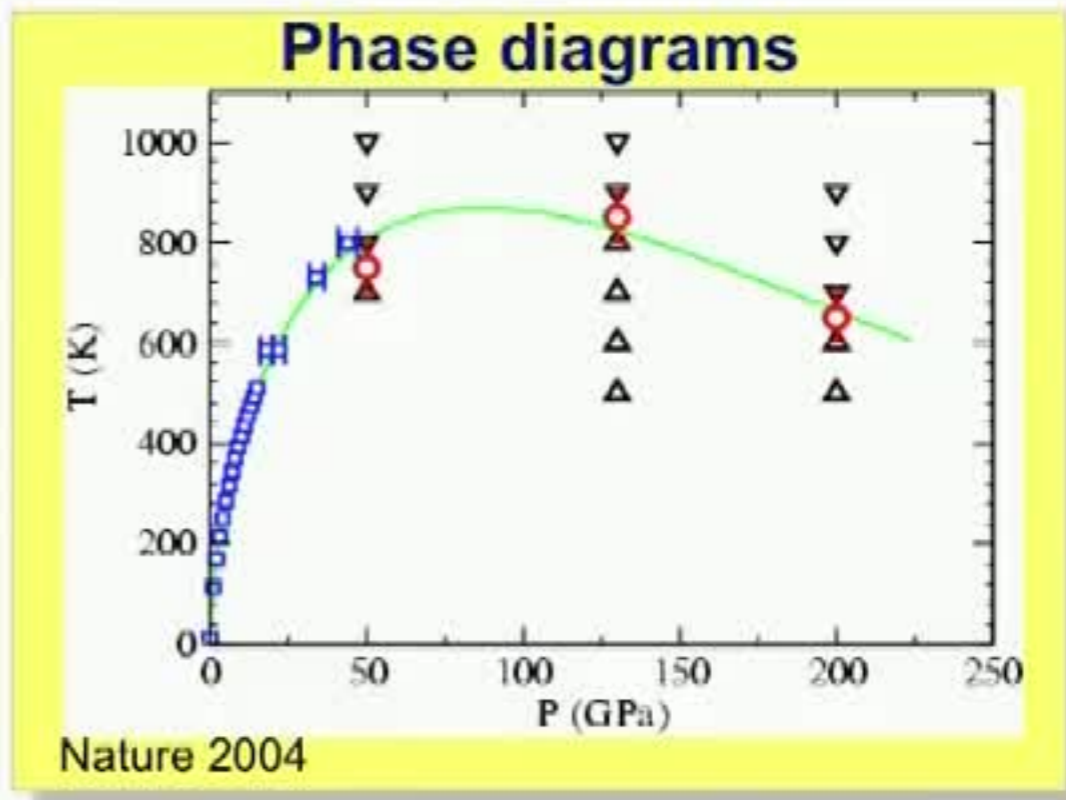


JPC-Lett. 2017

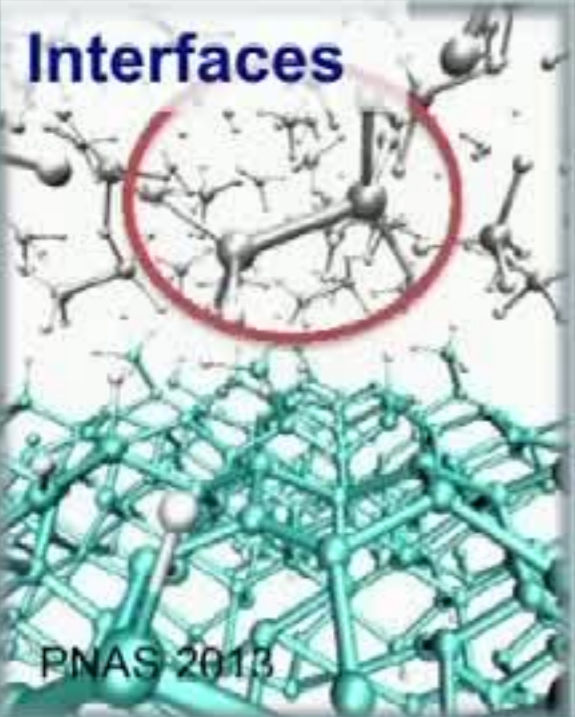
PNAS 2018

Nature Comm. 2018

This block contains three images related to liquid research. The top image shows a molecular simulation of a liquid with a water droplet splash, labeled 'JPC-Lett. 2017'. The middle image shows a molecular simulation of a liquid with a water droplet splash, labeled 'PNAS 2018'. The bottom image shows a molecular simulation of a liquid with a water droplet splash, labeled 'Nature Comm. 2018'.



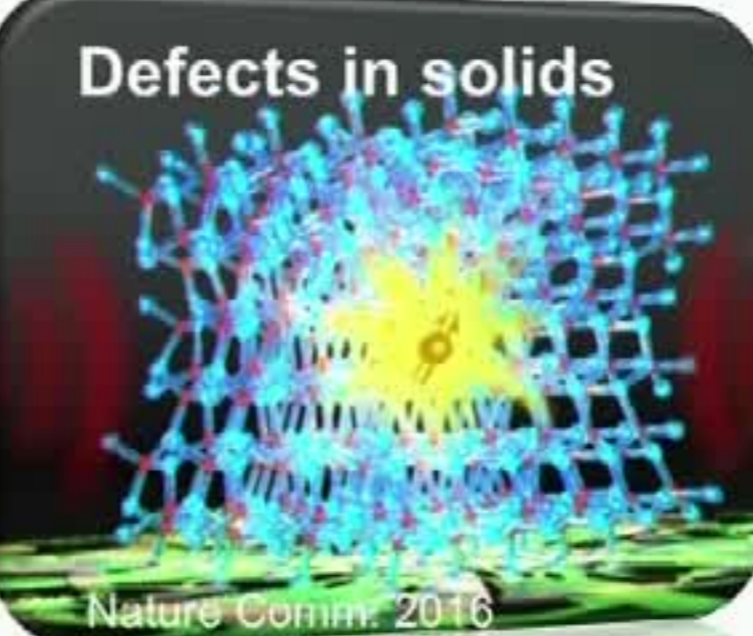
Interfaces



PNAS 2013

This image shows a molecular simulation of an interface between two materials. The top part shows a network of grey and white spheres, while the bottom part shows a network of green and white spheres. A red circle highlights a specific region at the interface.

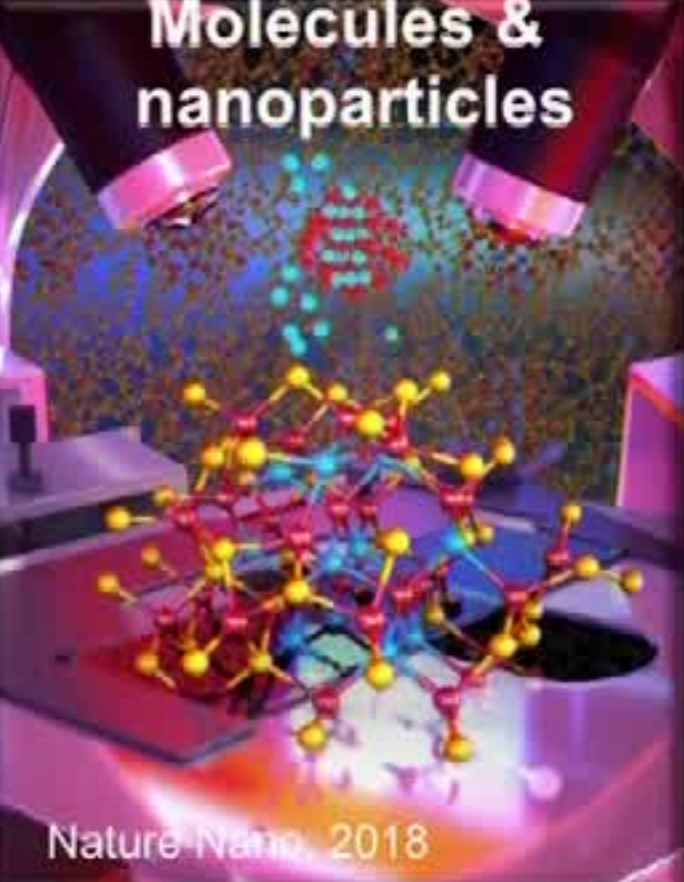
Defects in solids



Nature Comm. 2016

This image shows a molecular simulation of a defect in a solid lattice. The lattice is composed of blue and red spheres, with a central region highlighted in yellow, indicating the location of the defect.

Molecules & nanoparticles

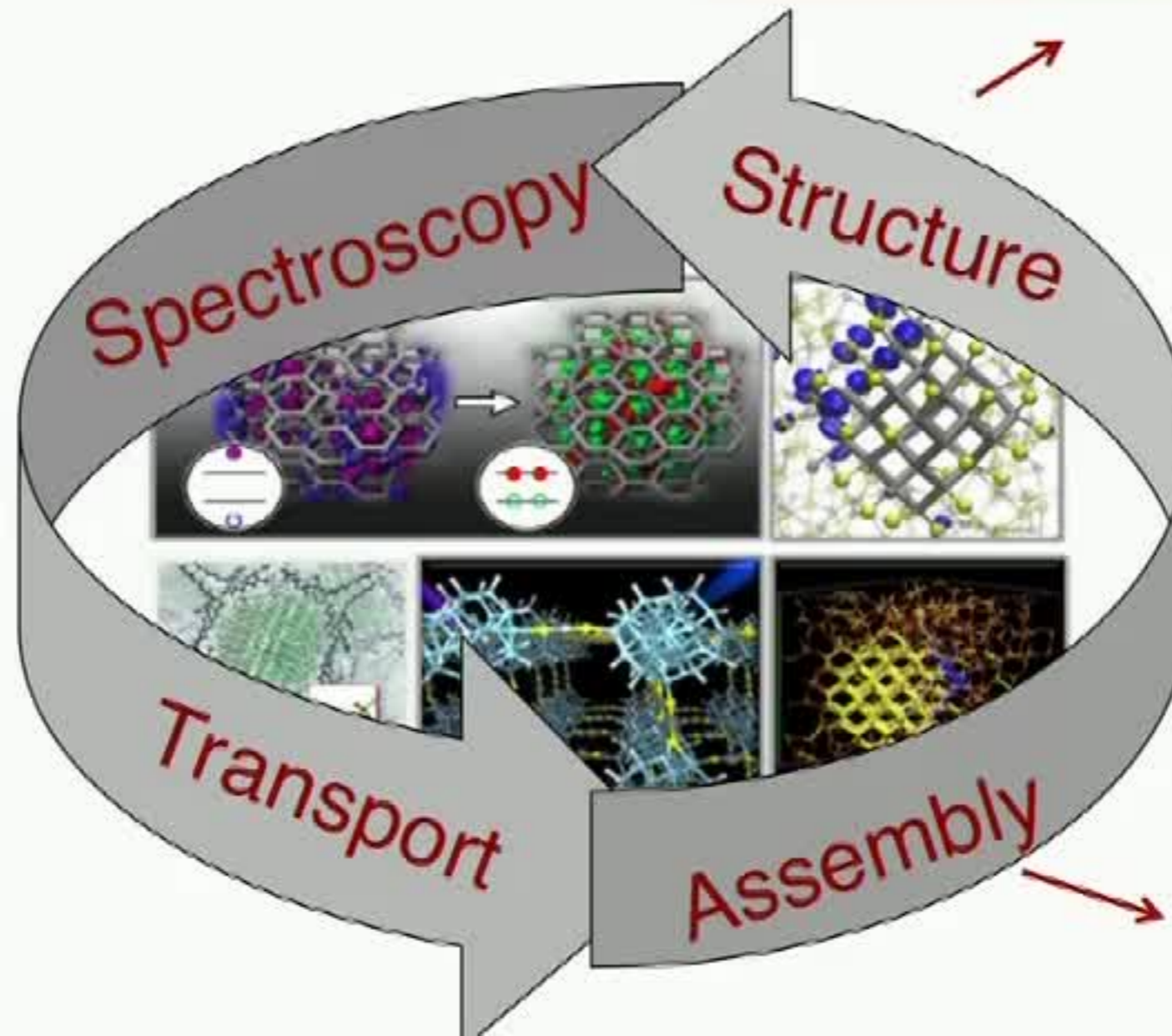


Nature Nano. 2018

This image shows a molecular simulation of molecules and nanoparticles. The molecules are represented by red and blue spheres, and the nanoparticles are represented by yellow and red spheres. The simulation is set against a background of a laboratory environment.

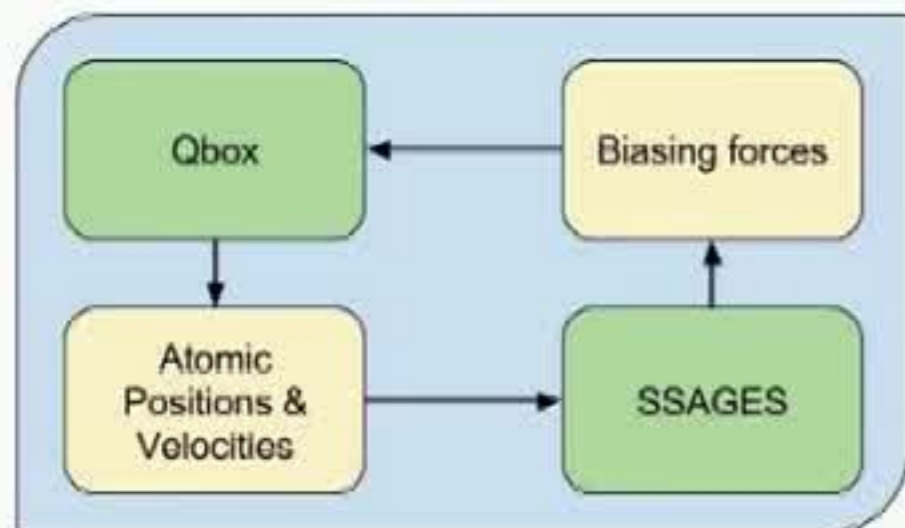
Integrated predictions of multiple properties

Geometrical arrangements of atoms; thermodynamic properties from approximate solutions of the **Schrodinger equation**



Advanced sampling techniques to assemble components/constituents out of equilibrium

Advanced sampling and ab initio MD

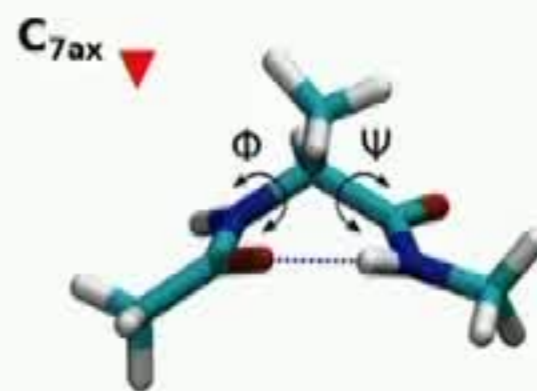
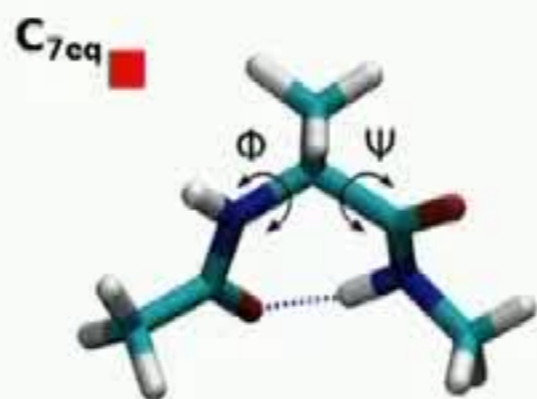
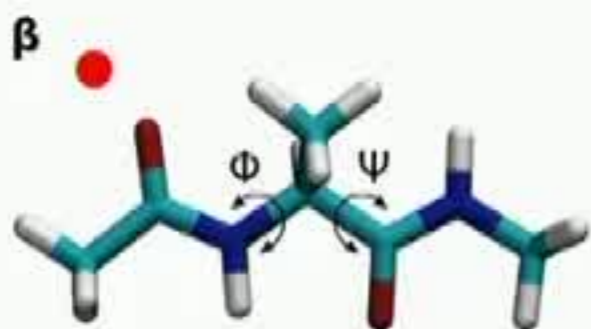


Qbox-SSAGES: Advanced sampling coupled with first-principles MD with DFT and hybrid DFT

Whitmer-Gygi-de Pablo-Galli collaboration
JCTC 2018

The coupled **Qbox-SSAGES** framework permits a hierarchical coupling. High level of theory (hybrid-functional) calculations can be restarted from previously converged lower level of theory (GGA) calculations.

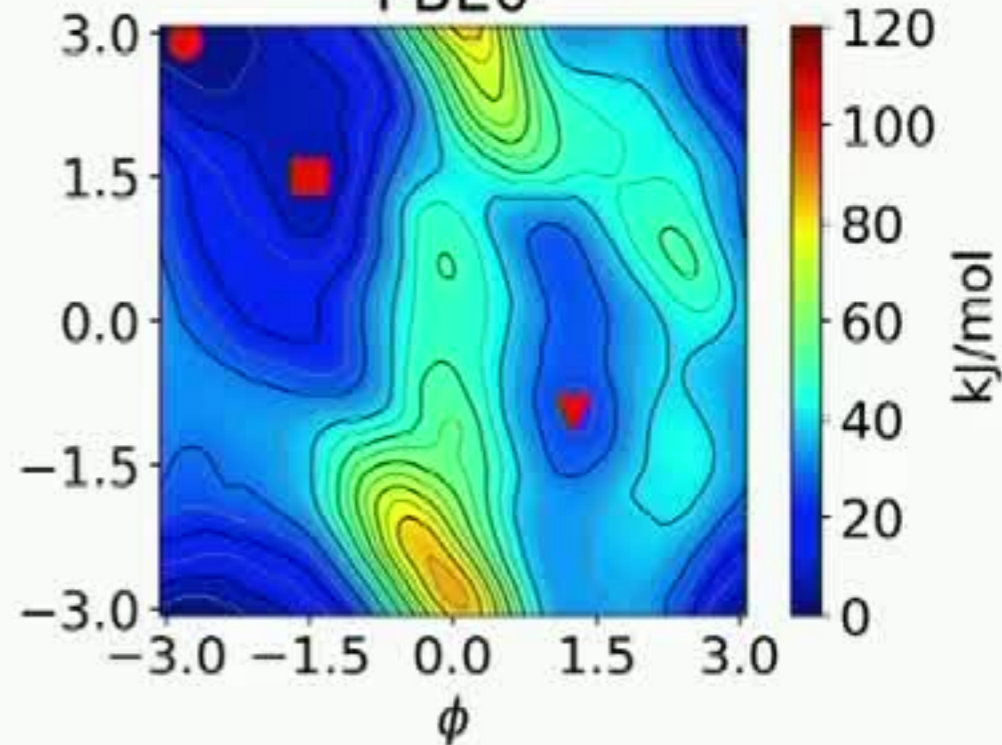
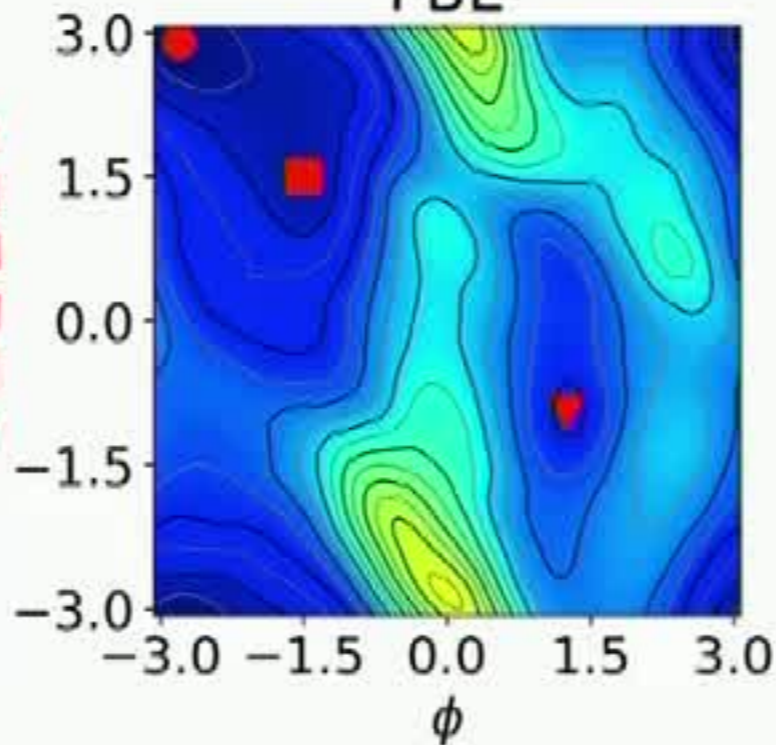
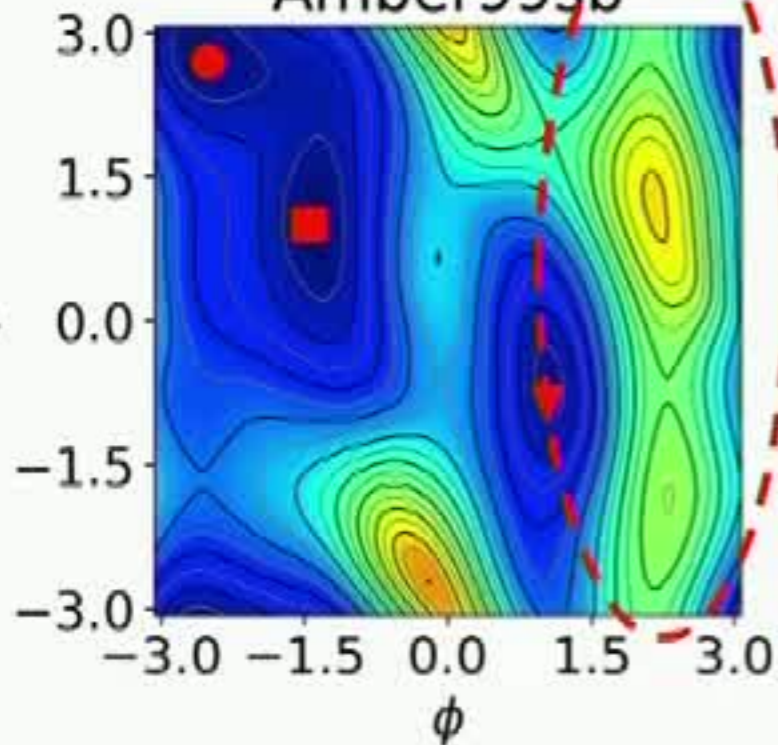
Free energy calculations of a peptide



Amber99sb

PBE

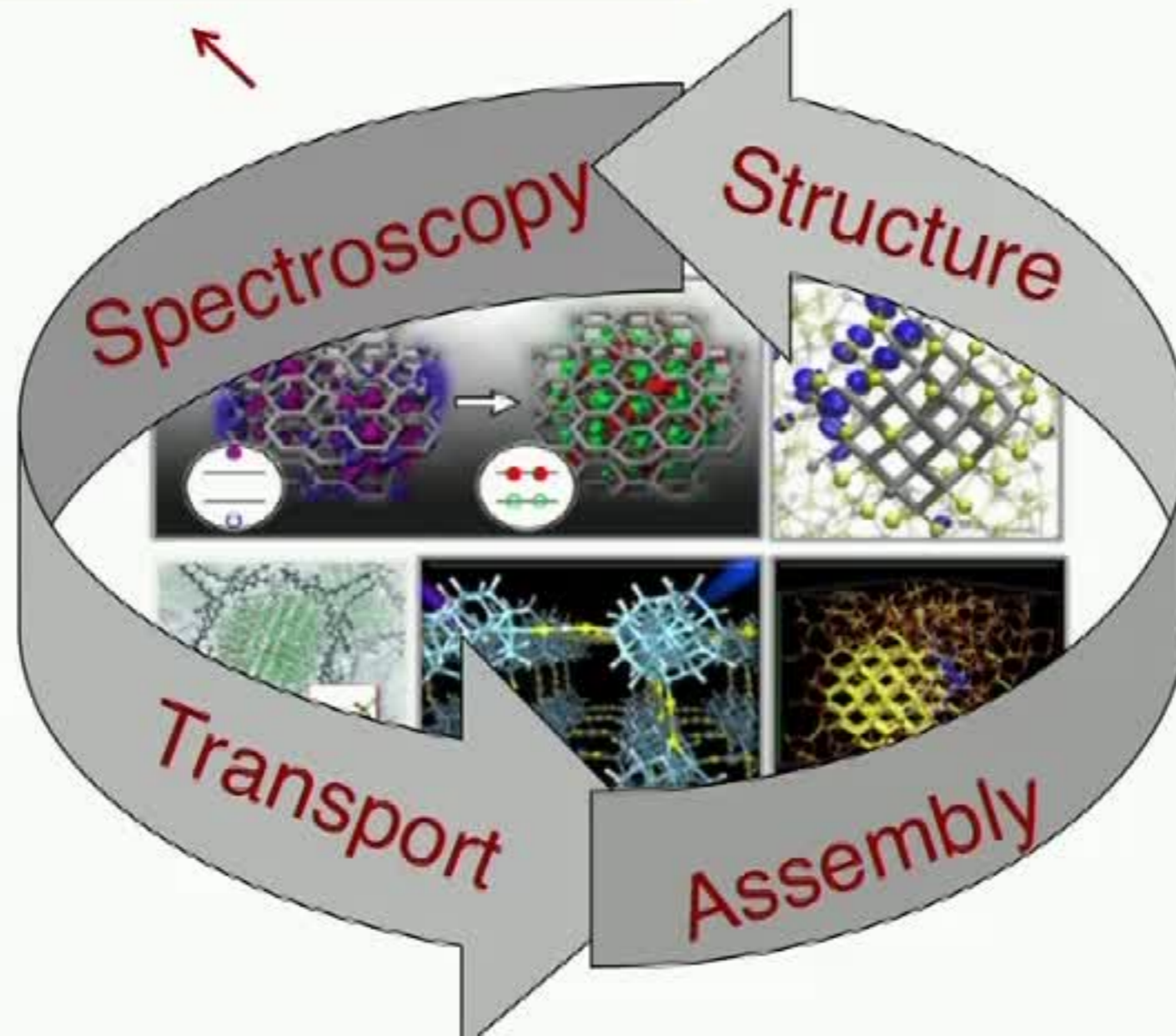
PBE0



Significant deviation in the free energy surfaces obtained at the DFT level (PBE and PBE0) from that calculated with **Amber99sb**

Integrated predictions of multiple properties

Interaction with electromagnetic fields (light) from the **coupling of Maxwell and Schroedinger equations** using linear response and perturbation theory



Spectroscopy on “MD samples”

Use trajectories to compute **complex electronic properties** from **many body perturbation (MBPT)** theory → Electronic properties at **finite T w/statistical errors**

$$\left(\hat{T} + \hat{V}_{ion} + \hat{V}_H + \hat{V}_{xc} \right) |\psi_n\rangle = \epsilon_n |\psi_n\rangle$$

DFT

$$\left(\hat{T} + \hat{V}_{ion} + \hat{V}_H + \hat{\Sigma}(E_n^{QP}) \right) |\psi_n^{QP}\rangle = E_n^{QP} |\psi_n^{QP}\rangle$$

MBPT

H. Wilson, F. Gygi, and G. G., PRB 2008; H.Wilson, D.Lu, F.Gygi and G.G., Phys.Rev.B 2009

H. V. Nguyen, T.A. Pham, D.Rocca and GG Phys. Rev. B (R) 2012; T.A.Pham, H.V.Nguyen, D.Rocca and GG, Phys.Rev.B 2013

M.Govoni & GG, J. Chem. Theory Comput., (2015); P.Scherpelz, I.Hamada, M.Govoni and GG, JCTC (2017); M.Govoni and GG, JCTC 2018

Maxwell equations for the external field

- $\mathbf{D} = \mathbf{E} + 4\pi\mathbf{P}$ \mathbf{D} = external field, independent of the material

$$\begin{aligned} \nabla \cdot \mathbf{D} &= 4\pi Q n_{\text{ext}} & \nabla \times \mathbf{E}(t) &= -\frac{1}{c} \frac{d\mathbf{B}}{dt} \\ \nabla \cdot \mathbf{B} &= 0 & \nabla \times \mathbf{B}(t) &= \frac{4\pi}{c} \mathbf{j}_{\text{ext}} + \frac{1}{c} \frac{d\mathbf{D}}{dt} \end{aligned}$$

- Relation between current and **total field** and density and **total field**

$$\mathbf{j}_{\text{int}}(\mathbf{r}, t) = \int d\mathbf{r}' \int^t \sigma(\mathbf{r}, \mathbf{r}', t - t') \mathbf{E}(\mathbf{r}', t')$$

$$\mathbf{j}_{\text{int}}(\mathbf{r}, \omega) = \int d\mathbf{r}' \sigma(\mathbf{r}, \mathbf{r}', \omega) \mathbf{E}(\mathbf{r}', \omega)$$

$$\mathbf{D}(\mathbf{r}, \omega) = \int d\mathbf{r}' \epsilon(\mathbf{r}, \mathbf{r}', \omega) \mathbf{E}(\mathbf{r}', \omega)$$

$$\mathbf{E}(\mathbf{r}, \omega) = \int d\mathbf{r}' \epsilon^{-1}(\mathbf{r}, \mathbf{r}', \omega) \mathbf{D}(\mathbf{r}', \omega)$$

- Response to the **total field E**

$$\epsilon(\mathbf{r}, \mathbf{r}', \omega) = 1\delta(\mathbf{r} - \mathbf{r}') + \frac{4\pi i}{\omega} \sigma(\mathbf{r}, \mathbf{r}', \omega)$$

- Response to the **external field D**

$$\rightarrow \epsilon^{-1}(\mathbf{r}, \mathbf{r}', \omega)$$

Spectroscopy on “MD samples”

Use trajectories to compute complex electronic properties from **many body perturbation (MBPT)** theory → Electronic properties at finite T w/statistical errors

$$\left(\hat{T} + \hat{V}_{ion} + \hat{V}_H + \hat{V}_{xc} \right) |\psi_n\rangle = \epsilon_n |\psi_n\rangle \quad \text{DFT}$$

$$\left(\hat{T} + \hat{V}_{ion} + \hat{V}_H + \hat{\Sigma}(E_n^{QP}) \right) |\psi_n^{QP}\rangle = E_n^{QP} |\psi_n^{QP}\rangle \quad \text{MBPT}$$

H. Wilson, F. Gygi, and G. G., PRB 2008; H.Wilson, D.Lu, F.Gygi and G.G., Phys.Rev.B 2009

H. V. Nguyen, T.A. Pham, D.Rocca and GG Phys. Rev. B (R) 2012; T.A.Pham, H.V.Nguyen, D.Rocca and GG, Phys.Rev.B 2013

M.Govoni & GG, J. Chem. Theory Comput., (2015); P.Scherpelz, I.Hamada, M.Govoni and GG, JCTC (2017); M.Govoni and GG, JCTC 2018

Hedin equations

Hedin proposed to express Σ in terms of the **dynamically screened Coulomb potential**, instead of the bare Coulomb potential

$$\begin{aligned}(\hat{T} + \hat{V}_{ion} + \hat{V}_H + \hat{V}_{xc}) |\psi_n\rangle &= \epsilon_n |\psi_n\rangle && \text{DFT} \\(\hat{T} + \hat{V}_{ion} + \hat{V}_H + \hat{\Sigma}(E_n^{QP})) |\psi_n^{QP}\rangle &= E_n^{QP} |\psi_n^{QP}\rangle && \text{MBPT}\end{aligned}$$

$$\Sigma(\mathbf{r}, \mathbf{r}'; \omega) = \int \frac{d\omega'}{2\pi} G(\mathbf{r}, \mathbf{r}'; \omega + \omega') W(\mathbf{r}, \mathbf{r}'; \omega')$$

$$G(\mathbf{r}, \mathbf{r}'; \omega) = \langle \mathbf{r} | \frac{1}{\omega - H} | \mathbf{r}' \rangle$$

$$W(\mathbf{r}, \mathbf{r}'; \omega) = \int d\mathbf{r}'' \epsilon^{-1}(\mathbf{r}, \mathbf{r}''; \omega) v_c(\mathbf{r}'', \mathbf{r}')$$

Use an expression in terms of Kohn-Sham electronic states from density-density response functions

$$E_n^{QP} = \epsilon_n^{KS} + \langle \psi_n^{KS} | \hat{\Sigma}(E_n^{QP}) - \hat{V}_{xc} | \psi_n^{KS} \rangle$$

Calculations of dielectric matrices: spectral decomposition & DFPT

$$\tilde{\epsilon}^{-1} = \sum_{i=1}^{\text{Neig}} \tilde{\phi}_i \left(\frac{\lambda_i}{1 - \lambda_i} + 1 \right) \tilde{\phi}_i^H$$

- Calculation of **empty electronic states**, calculation and storage of **full dielectric matrix** and **inversion** of $\tilde{\epsilon}$ are **avoided**
- **Scaling**: $N_{\text{eig}} N_{\text{pw}} N_v^2$ (instead of $N_{\text{pw}}^2 N_v N_c$)
- Efficient evaluation of $\tilde{\epsilon}^{-1}$ at different \mathbf{q} points and at different MD steps is possible
- Incorporation of XC kernel is in principle straightforward

Hedin equations

Hedin proposed to express Σ in terms of the **dynamically screened Coulomb potential**, instead of the bare Coulomb potential

$$\begin{aligned} (\hat{T} + \hat{V}_{ion} + \hat{V}_H + \hat{V}_{xc}) |\psi_n\rangle &= \epsilon_n |\psi_n\rangle && \text{DFT} \\ (\hat{T} + \hat{V}_{ion} + \hat{V}_H + \hat{\Sigma}(E_n^{QP})) |\psi_n^{QP}\rangle &= E_n^{QP} |\psi_n^{QP}\rangle && \text{MBPT} \end{aligned}$$

$$\Sigma(\mathbf{r}, \mathbf{r}'; \omega) = \int \frac{d\omega'}{2\pi} G(\mathbf{r}, \mathbf{r}'; \omega + \omega') W(\mathbf{r}, \mathbf{r}'; \omega')$$

$$G(\mathbf{r}, \mathbf{r}'; \omega) = \langle \mathbf{r} | \frac{1}{\omega - H} | \mathbf{r}' \rangle$$

$$W(\mathbf{r}, \mathbf{r}'; \omega) = \int d\mathbf{r}'' \epsilon^{-1}(\mathbf{r}, \mathbf{r}''; \omega) v_c(\mathbf{r}'', \mathbf{r}')$$

Use an expression in terms of Kohn-Sham electronic states from density-density response functions

$$E_n^{QP} = \epsilon_n^{KS} + \langle \psi_n^{KS} | \hat{\Sigma}(E_n^{QP}) - \hat{V}_{xc} | \psi_n^{KS} \rangle$$

Calculations of dielectric matrices: spectral decomposition & DFPT

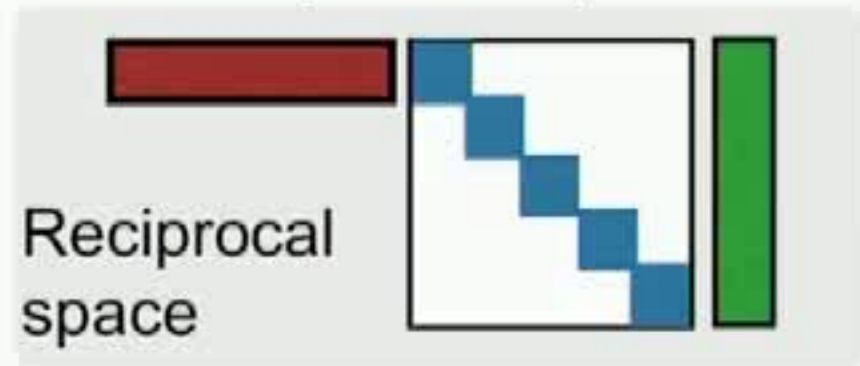
$$\tilde{\epsilon}^{-1} = \sum_{i=1}^{\text{Neig}} \tilde{\phi}_i \left(\frac{\lambda_i}{1 - \lambda_i} + 1 \right) \tilde{\phi}_i^H$$

- Calculation of **empty electronic states**, calculation and storage of **full dielectric matrix** and **inversion** of $\tilde{\epsilon}$ are **avoided**
- **Scaling**: $N_{\text{eig}} N_{\text{pw}} N_v^2$ (instead of $N_{\text{pw}}^2 N_v N_c$)
- Efficient evaluation of $\tilde{\epsilon}^{-1}$ at different \mathbf{q} points and at different MD steps is possible
- Incorporation of XC kernel is in principle straightforward

Low rank decomposition of the screened Coulomb interaction W

In **Hartree-Fock**

$$\langle \psi_i \psi_j | \frac{1}{|\mathbf{r} - \mathbf{r}'|} | \psi_k \psi_l \rangle$$



In **GW**

$$\langle \psi_i \psi_j | W(\mathbf{r}, \mathbf{r}') | \psi_k \psi_l \rangle$$



$$W = \sum_{\alpha} |\alpha\rangle \lambda_{\alpha} \langle \alpha|$$

Low-rank decomposition



Calculations of dielectric matrices: spectral decomposition & DFPT

$$\tilde{\epsilon}^{-1} = \sum_{i=1}^{\text{Neig}} \tilde{\phi}_i \left(\frac{\lambda_i}{1 - \lambda_i} + 1 \right) \tilde{\phi}_i^H$$

- Calculation of **empty electronic states**, calculation and storage of **full dielectric matrix** and **inversion** of $\tilde{\epsilon}$ are **avoided**
- **Scaling**: $N_{\text{eig}} N_{\text{pw}} N_v^2$ (instead of $N_{\text{pw}}^2 N_v N_c$)
- Efficient evaluation of $\tilde{\epsilon}^{-1}$ at different \mathbf{q} points and at different MD steps is possible
- Incorporation of XC kernel is in principle straightforward

Hedin equations

Hedin proposed to express Σ in terms of the **dynamically screened Coulomb potential**, instead of the bare Coulomb potential

$$\begin{aligned}(\hat{T} + \hat{V}_{ion} + \hat{V}_H + \hat{V}_{xc}) |\psi_n\rangle &= \epsilon_n |\psi_n\rangle && \text{DFT} \\(\hat{T} + \hat{V}_{ion} + \hat{V}_H + \hat{\Sigma}(E_n^{QP})) |\psi_n^{QP}\rangle &= E_n^{QP} |\psi_n^{QP}\rangle && \text{MBPT}\end{aligned}$$

$$\Sigma(\mathbf{r}, \mathbf{r}'; \omega) = \int \frac{d\omega'}{2\pi} G(\mathbf{r}, \mathbf{r}'; \omega + \omega') W(\mathbf{r}, \mathbf{r}'; \omega')$$

$$G(\mathbf{r}, \mathbf{r}'; \omega) = \langle \mathbf{r} | \frac{1}{\omega - H} | \mathbf{r}' \rangle$$

$$W(\mathbf{r}, \mathbf{r}'; \omega) = \int d\mathbf{r}'' \epsilon^{-1}(\mathbf{r}, \mathbf{r}''; \omega) v_c(\mathbf{r}'', \mathbf{r}')$$

Use an expression in terms of Kohn-Sham electronic states from density-density response functions

$$E_n^{QP} = \epsilon_n^{KS} + \langle \psi_n^{KS} | \hat{\Sigma}(E_n^{QP}) - \hat{V}_{xc} | \psi_n^{KS} \rangle$$

Calculations of dielectric matrices: spectral decomposition & DFPT

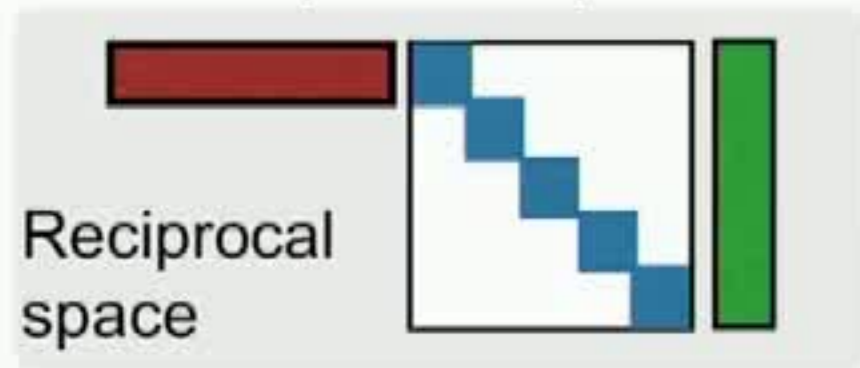
$$\tilde{\epsilon}^{-1} = \sum_{i=1}^{\text{Neig}} \tilde{\phi}_i \left(\frac{\lambda_i}{1 - \lambda_i} + 1 \right) \tilde{\phi}_i^H$$

- Calculation of **empty electronic states**, calculation and storage of **full dielectric matrix** and **inversion** of $\tilde{\epsilon}$ are **avoided**
- **Scaling**: $N_{\text{eig}} N_{\text{pw}} N_v^2$ (instead of $N_{\text{pw}}^2 N_v N_c$)
- Efficient evaluation of $\tilde{\epsilon}^{-1}$ at different \mathbf{q} points and at different MD steps is possible
- Incorporation of XC kernel is in principle straightforward

Low rank decomposition of the screened Coulomb interaction W

In **Hartree-Fock**

$$\langle \psi_i \psi_j | \frac{1}{|\mathbf{r} - \mathbf{r}'|} | \psi_k \psi_l \rangle$$



In **GW**

$$\langle \psi_i \psi_j | W(\mathbf{r}, \mathbf{r}') | \psi_k \psi_l \rangle$$



$$W = \sum_{\alpha} |\alpha\rangle \lambda_{\alpha} \langle \alpha|$$

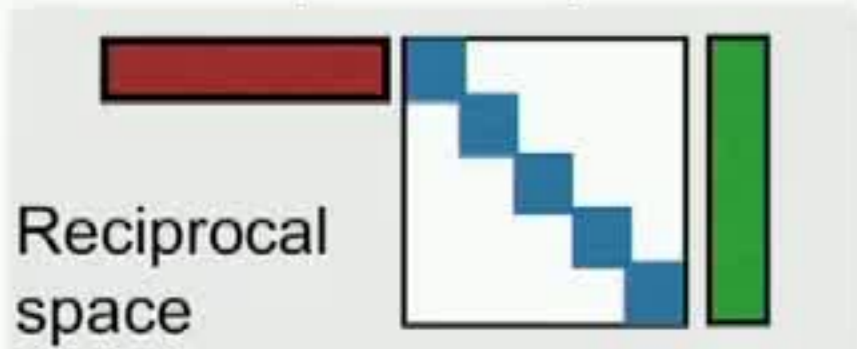
Low-rank decomposition



Low rank decomposition of the screened Coulomb interaction W

In **Hartree-Fock**

$$\langle \psi_i \psi_j | \frac{1}{|\mathbf{r} - \mathbf{r}'|} | \psi_k \psi_l \rangle$$



In **GW**

$$\langle \psi_i \psi_j | W(\mathbf{r}, \mathbf{r}') | \psi_k \psi_l \rangle$$



Example : 64 water molecules

Direct space	size $\sim (250)^3 \times (250)^3$ Difficult to truncate
Reciprocal space	size $\sim (1'000'000) \times (1'000'000)$ Could be truncated, full matrix
Eigenpotential space	size $\sim (1'000) \times (1'000)$

$$W = \sum_{\alpha} |\alpha\rangle \lambda_{\alpha} \langle \alpha|$$

Low-rank decomposition



Summary of GW algorithm

- Iterative diagonalization of the dielectric matrix ⁽⁺⁾ →
- Low rank decomposition of W
- DFPT ^(*) based projection techniques to compute G
- Eigenpotentials of $\tilde{\epsilon}$ as basis set also at finite frequency ⁽⁺⁺⁾
- Lanczos algorithm to compute frequency dependence of dielectric matrix in parallel
- Contour deformation technique for frequency integration ^(&)

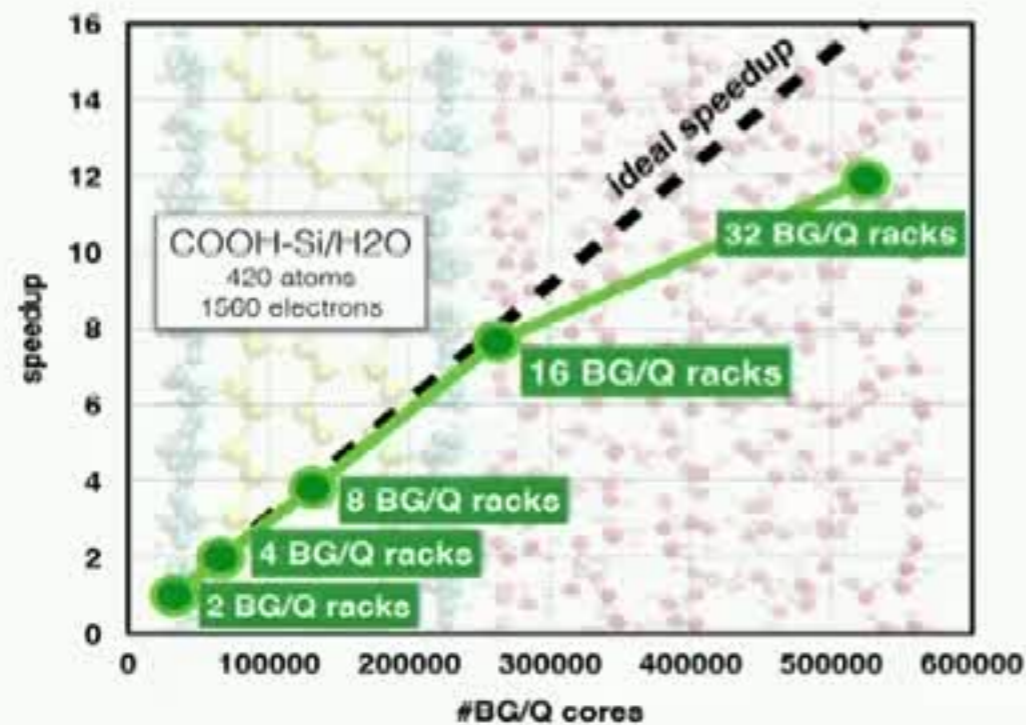
(*) S. Baroni, et al., Rev. Mod. Phys., 73:515, 2001.

(+) H. Wilson, F. Gygi, and G. G., PRB 2008; H.Wilson, D.Lu, F.Gygi and G.G., Phys.Rev.B 2009

(++) H. V. Nguyen, T.A. Pham, D.Rocca and GG Phys. Rev. B (R) 2012; T.A.Pham, H,V.Nguyen, D.Rocca and GG, Phys.Rev.B 2013

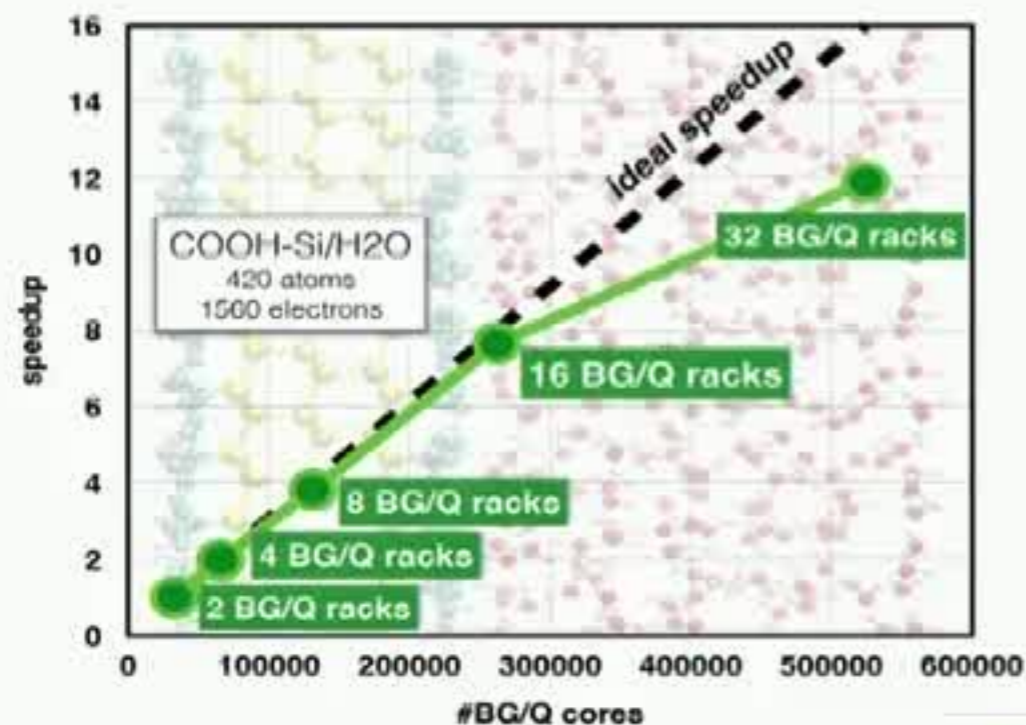
(&) M.Govoni & GG, J. Chem. Theory Comput., (2015)

Implementation of GW algorithm



- Eliminated summations over **empty states** using DFPT
- We made **separable** using the eigenvectors of the dielectric matrix as basis set; number of eigenpotentials controls the **accuracy** of the method.
- Greatly **reduced pre-factors** of $O(N^4)$ scaling

Implementation of GW algorithm



Range of applicability

Ordered and disordered **solids**,
defective materials, **liquids**,
molecular crystals,
nanostructures, interfaces



Govoni&GG, JCTC 2015, JCTC 2018

- Eliminated summations over **empty states** using DFPT
- We made **separable** using the eigenvectors of the dielectric matrix as basis set; number of eigenpotentials controls the **accuracy** of the method.
- Greatly **reduced pre-factors** of $O(N^4)$ scaling

Home What's New? Download Documentation Team Contacts Publications News

< WEST! >

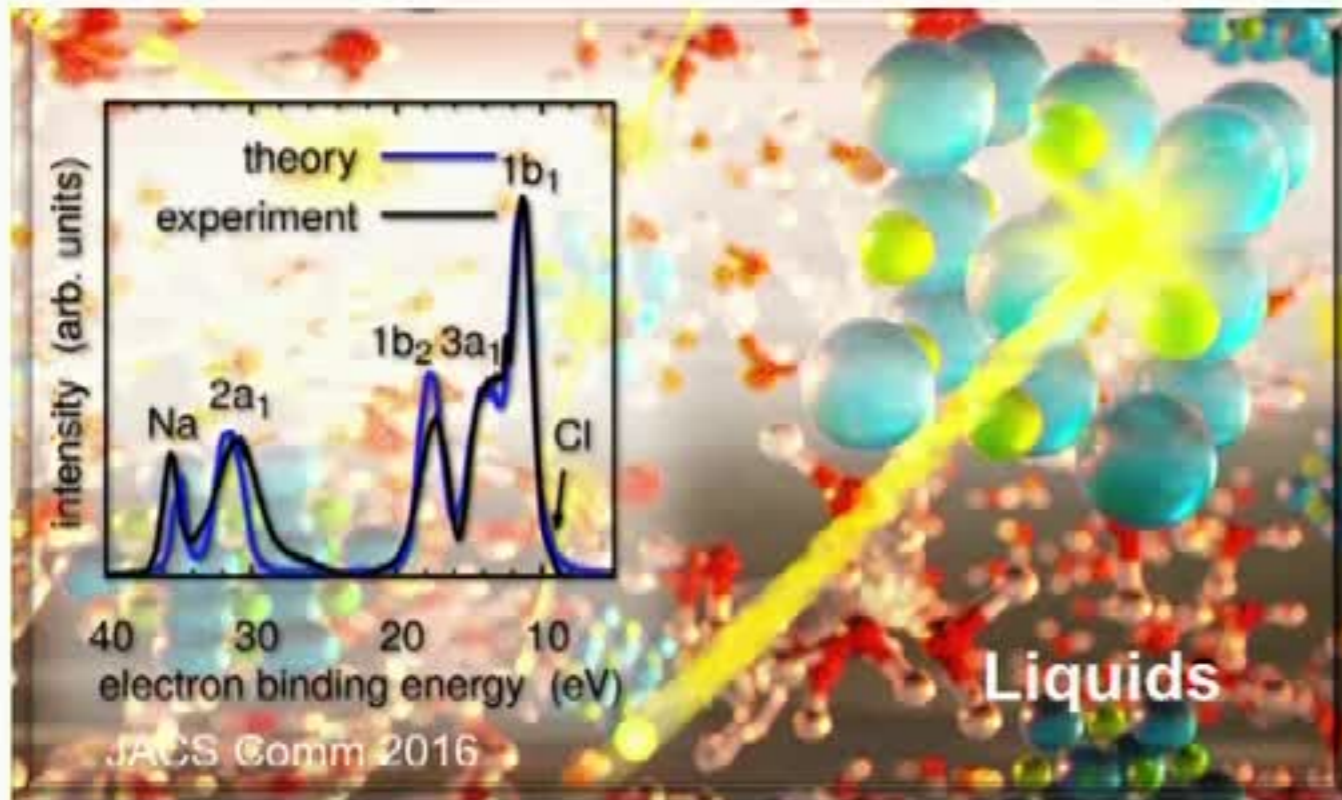
West is available for download under the GPL. [Get West!](#)



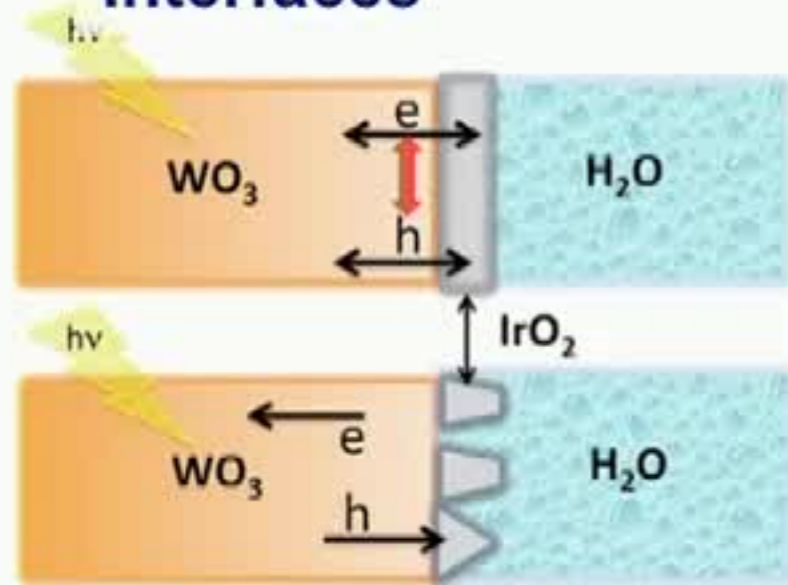
www.west-code.org

scalable to > 500,000 cores

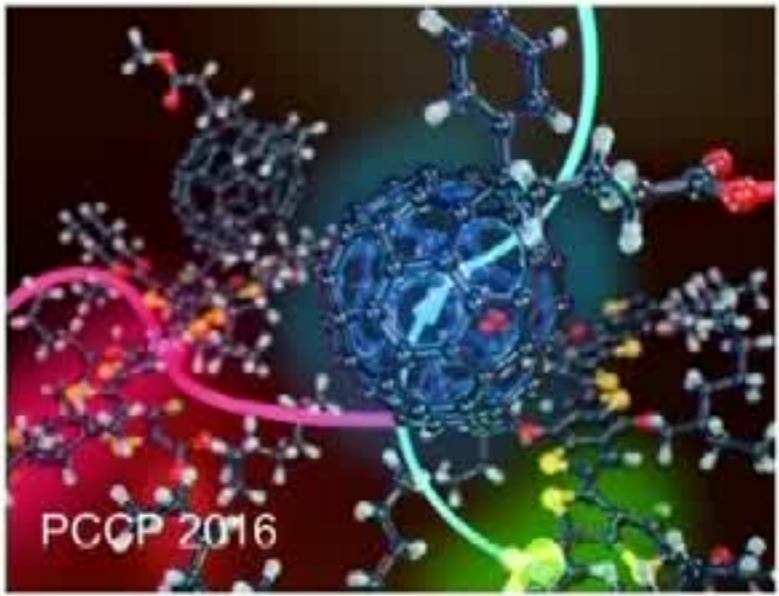
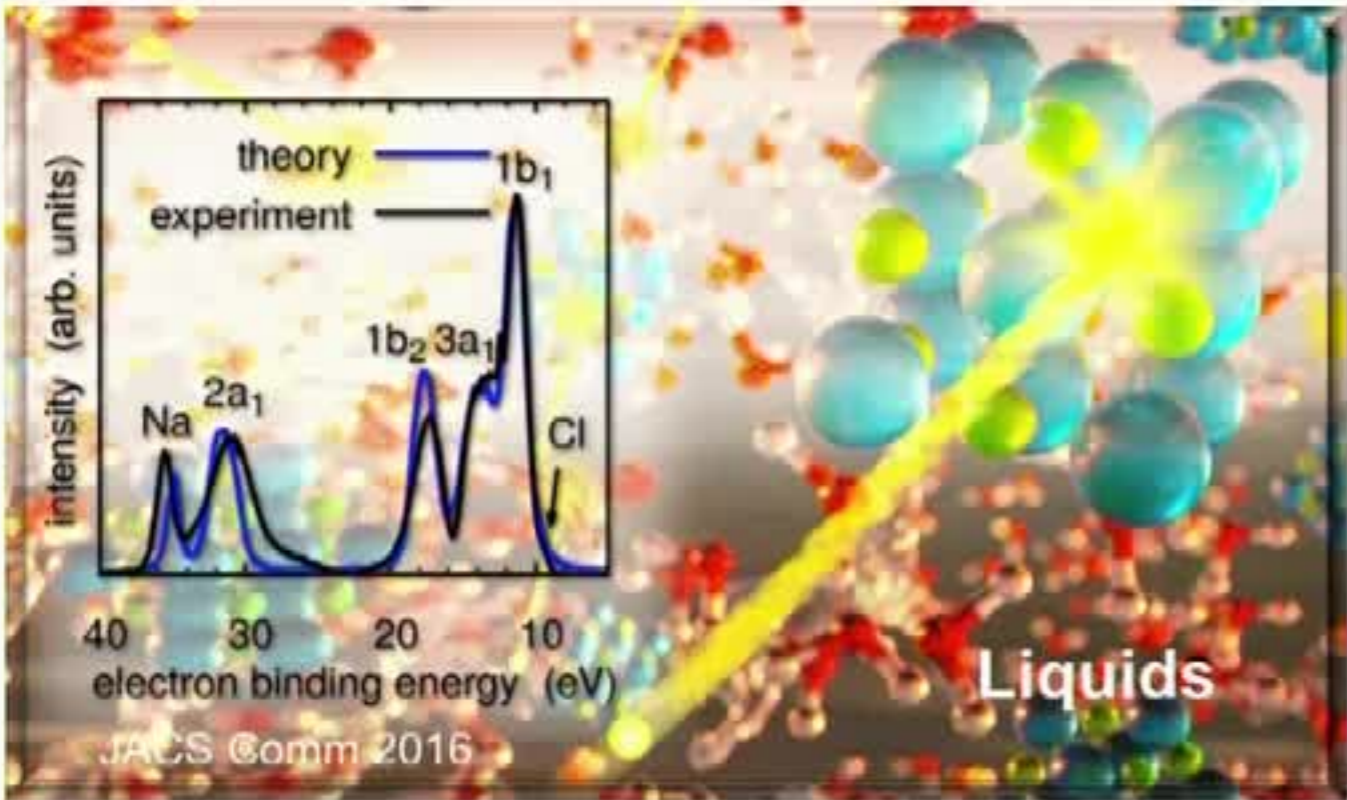
Some examples



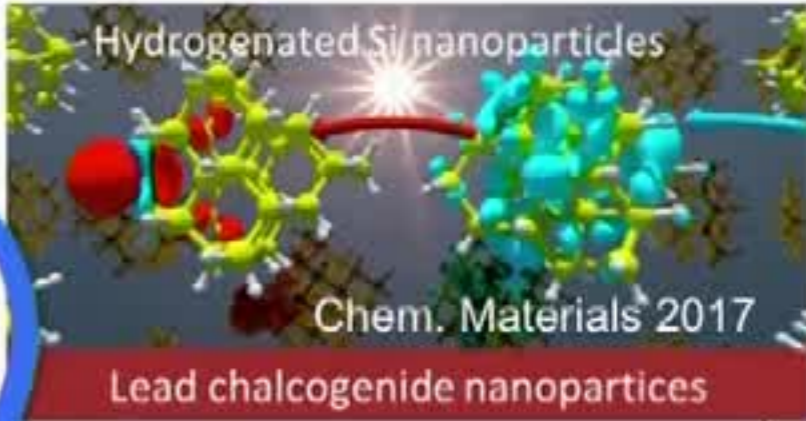
Interfaces



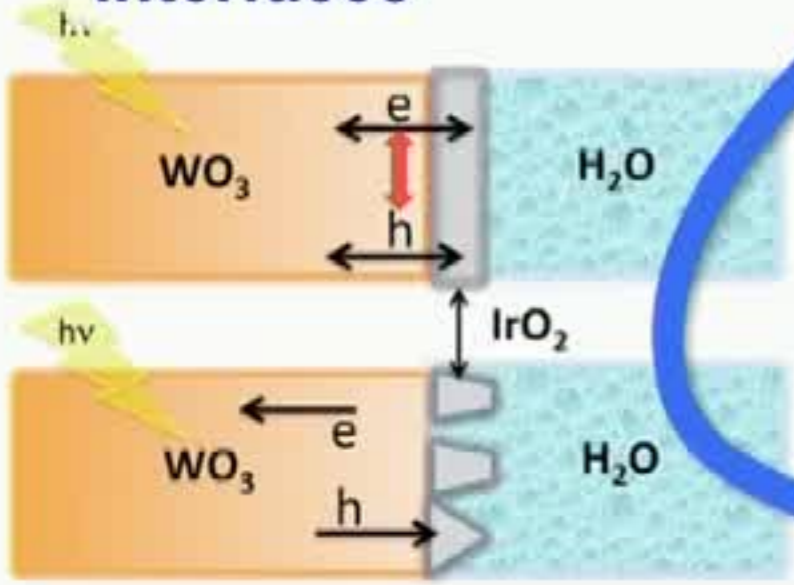
Some examples



Nanoparticles

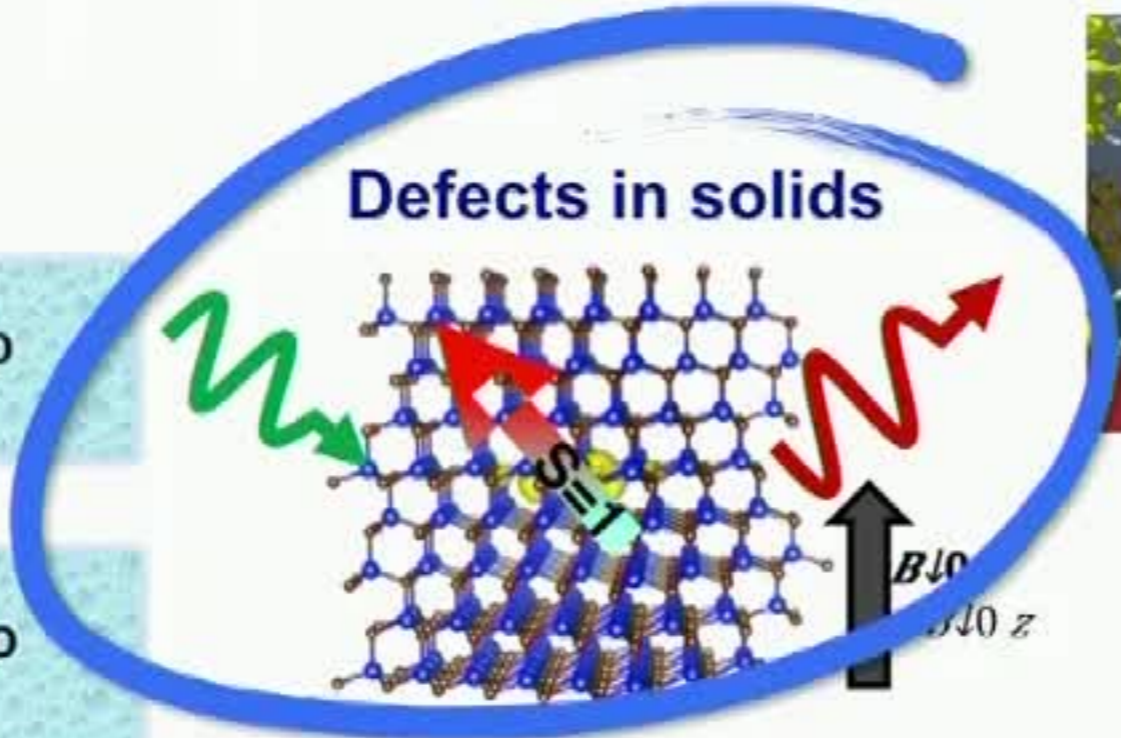


Interfaces



JACS Comm 2015

Defects in solids



Nature Comm. 2016

Absorption of light: solving the Bethe Salpeter equation (BSE)

Quantum Liouville equation

$$i \frac{d\hat{\rho}(t)}{dt} = [\hat{H}(t), \hat{\rho}(t)]$$

$$\hat{H}(t)\phi(\mathbf{r}, t) = \left[-\frac{1}{2}\nabla^2 + v_H(\mathbf{r}, t) + v_{ext}(\mathbf{r}, t) \right] \phi(\mathbf{r}, t) + \int \Sigma(\mathbf{r}, \mathbf{r}', t) \phi(\mathbf{r}', t) d\mathbf{r}'$$

$$\Sigma_{COH}(\mathbf{r}, \mathbf{r}') = \frac{1}{2} \delta(\mathbf{r} - \mathbf{r}') W_p(\mathbf{r}', \mathbf{r}) \quad \text{BSE}$$

$$\Sigma_{SEX}(\mathbf{r}, \mathbf{r}', t) = - \sum_v \phi_v(\mathbf{r}, t) \phi_v^*(\mathbf{r}', t) W(\mathbf{r}', \mathbf{r})$$

Screened Coulomb interaction

- The quantum Liouville equation is solved within linear response theory
- Explicit calculation of empty electronic states is avoided by using iterative diag. of ε
- The Tamm-Dancoff approximation is not necessary

D. Rocca, D. Lu, and G. Galli, *JCP* (2010)
D. Rocca, Y. Ping, R. Gebauer, and G. Galli, *PRB* (2012)

D. Rocca, R. Gebauer, Y. Saad, and S. Baroni, *JCP* (2008)
B. Walker, R. Gebauer, A. M. Saitta, and S. Baroni, *PRL* (2006)

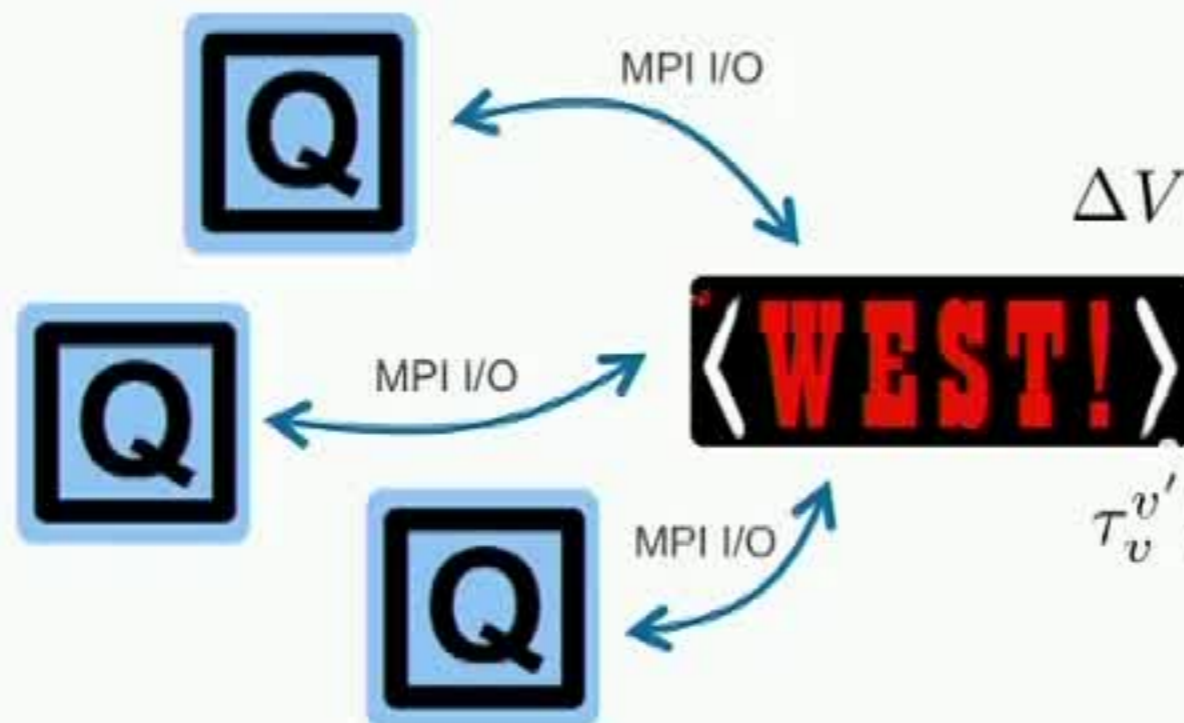
Finite field calculations to solve the Bethe Salpeter equation

$$K_{v,v'}^{1d} |a_{v'}\rangle = \hat{P}_c \left(\int \mathbf{W}(\mathbf{r}, \mathbf{r}') \varphi_{v'}^{o*}(\mathbf{r}') \varphi_v^o(\mathbf{r}') d\mathbf{r}' \right) |a_{v'}\rangle$$

$$\hat{\mathbf{W}} = \mathbf{v}_c + \mathbf{v}_c \chi \mathbf{v}_c$$

$$\hat{H} = \hat{H}_o + \Delta V(r)$$

$$\Delta\rho(r) = \sum_v \varphi_v^{o*}(r) \times [\varphi_v(r) - \varphi_v^o(r)]$$



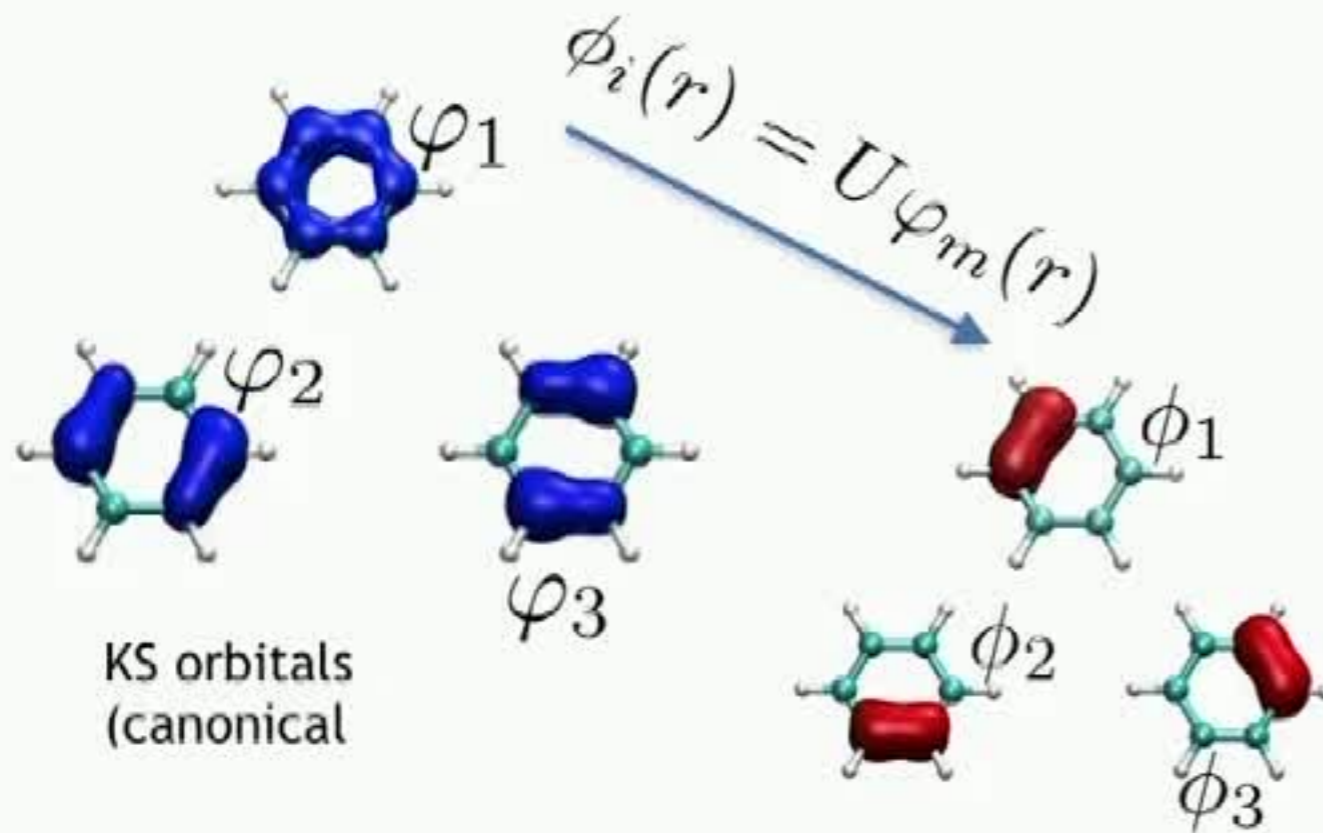
$$\Delta V(r) = \int \mathbf{v}_c(\mathbf{r}, \mathbf{r}') \rho_v^{v'}(r') dr'$$

$$\begin{aligned} \tau_v^{v'}(r) &= \int \hat{\mathbf{W}}(\mathbf{r}, \mathbf{r}') \varphi_{v'}^*(r) \varphi_v(r) \\ &= \Delta V + \int v_c(r, r') \Delta\rho(r') dr' \end{aligned}$$

Reduction of scaling from N^4 to N^3

$$K_{v,v'}^{1d} |a_{v'}\rangle = \hat{\mathbf{P}}_c \left(\int \mathbf{W}(\mathbf{r}, \mathbf{r}') \underset{U^\dagger}{\varphi_{v'}^{o*}}(\mathbf{r}') \underset{U}{\varphi_v^o}(\mathbf{r}') d\mathbf{r}' \right) |a_{v'}\rangle$$

$$U^\dagger U = I$$

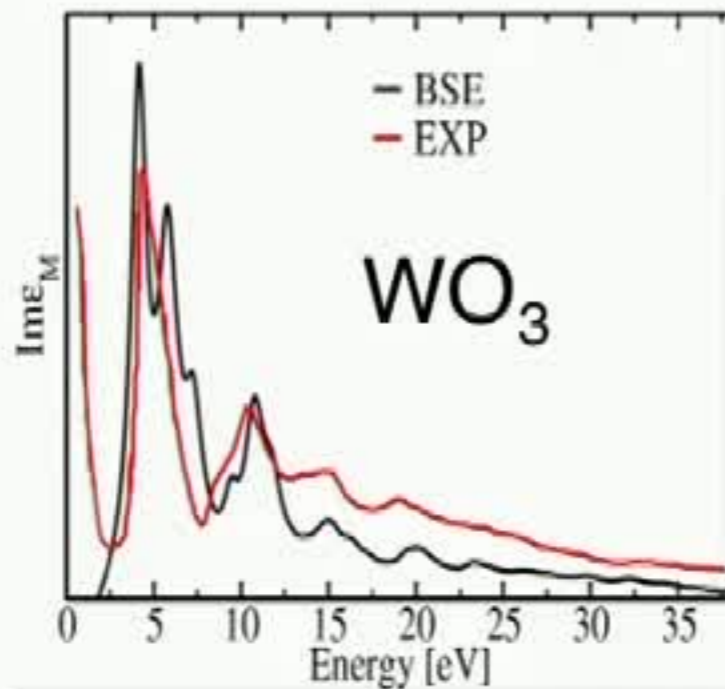


$$\varphi_1(r) \times \varphi_2(r) \neq 0$$

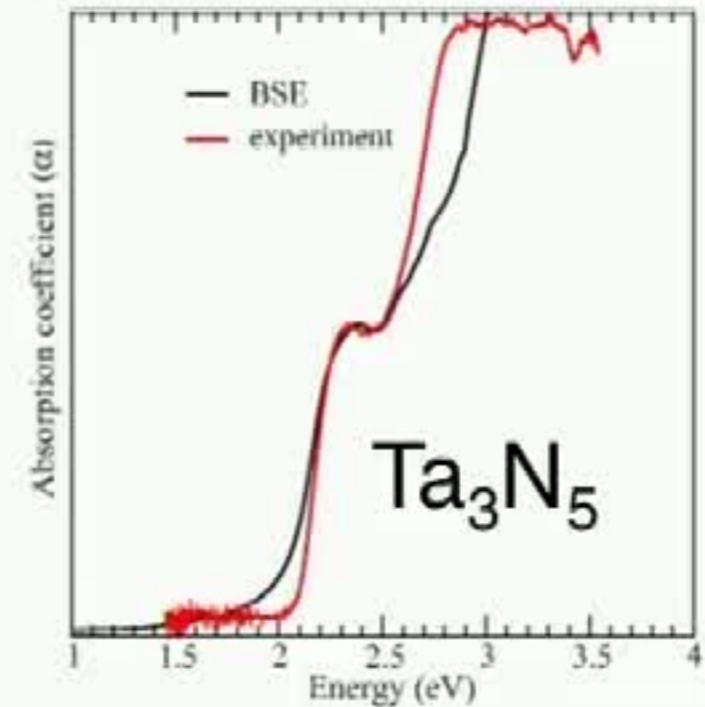
$$\phi_1(r) \times \phi_2(r) \sim 0$$

Some examples

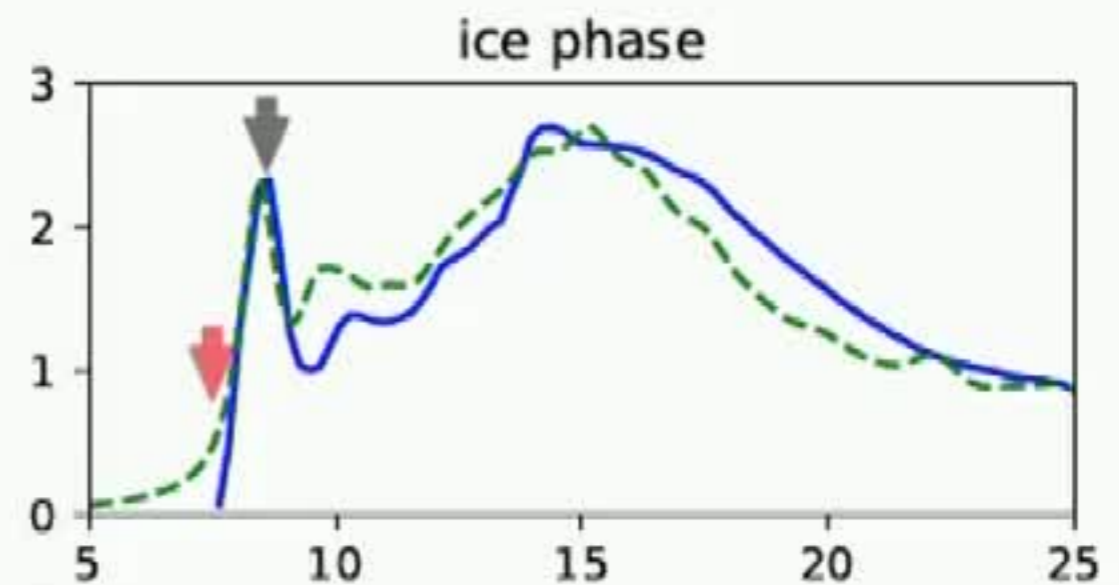
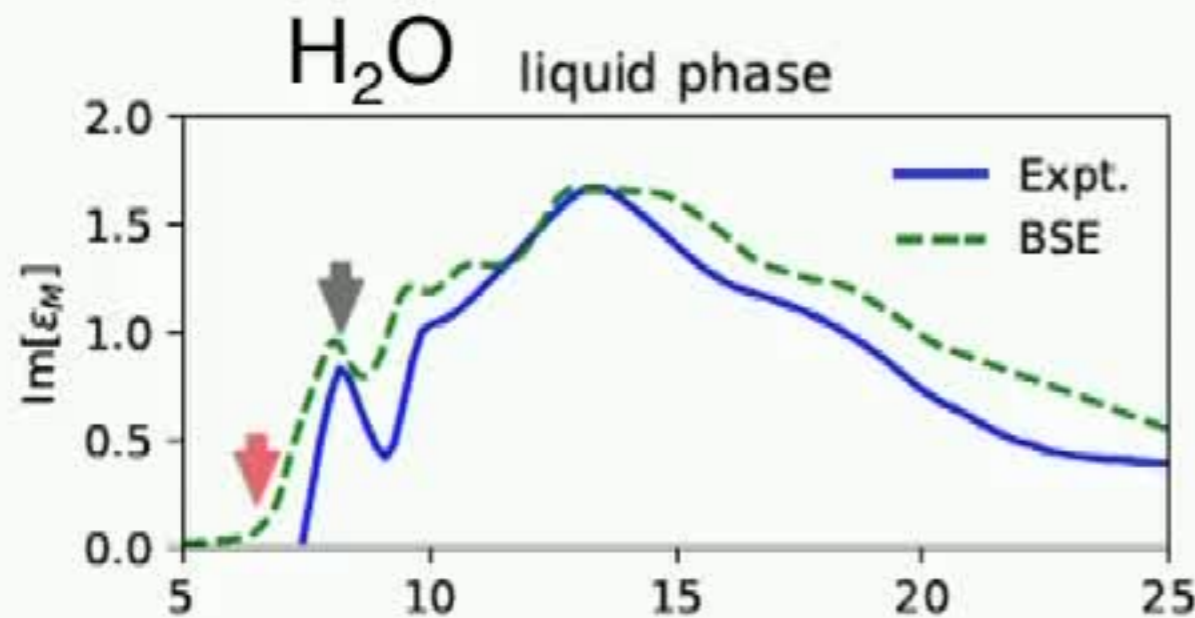
Absorption spectra: solids & liquids



PRB 2013;



PRB 2014 & 2016



Method developments & software interoperability

- **WEST**

- Many-body perturb. theory

- <http://www.west-code.org>

- **Qbox**

- First-principles MD

- <http://qboxcode.org>

- **SSAGES**

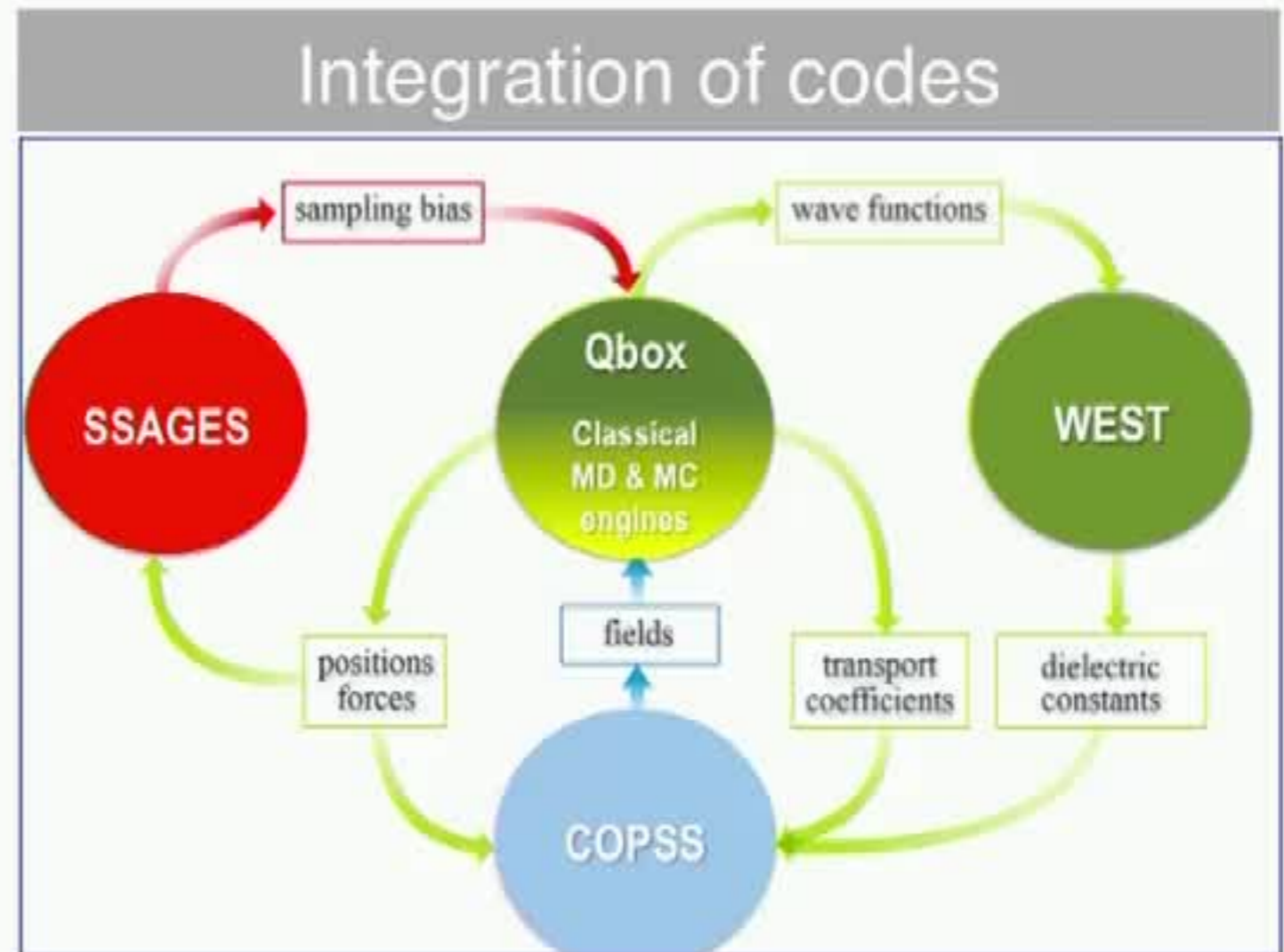
- Advanced sampling

- <http://miccomcodes.org/>

- **COPSS**

- Particle-continuum codes

- <http://miccomcodes.org/>

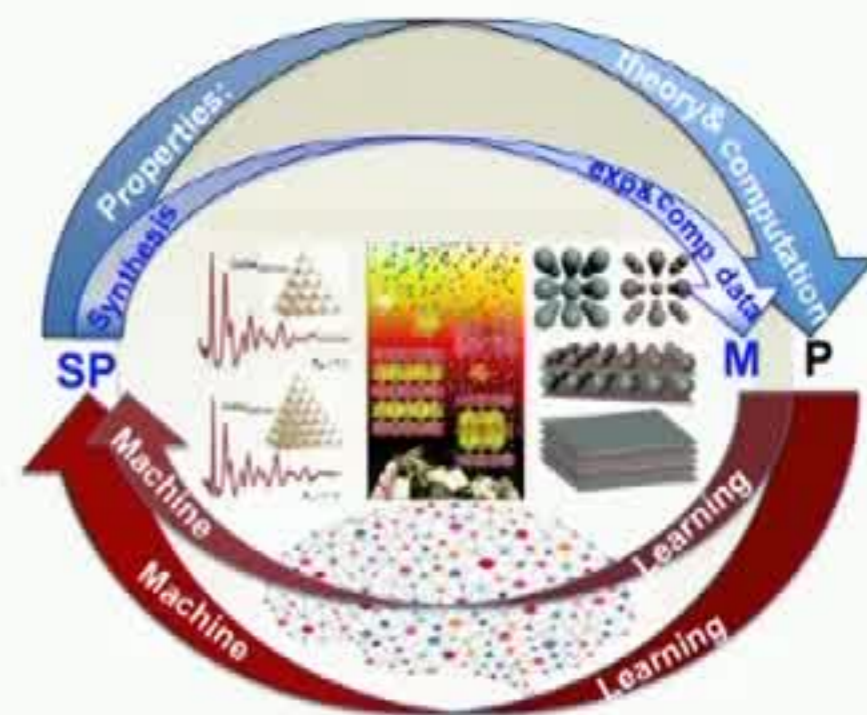


<http://miccom-center.org/software.html>

Discovery & Design

- ‘Inverse problems’ : not yet there

—The road to progress will include the ability to carry out *robust & efficient* calculations of *many materials properties*



- Predictions on how to **synthesize** a material with **desired properties**: not yet there

—Computational synthesis requires brand new theoretical and computational strategies

- **Discovery of new physical phenomena**

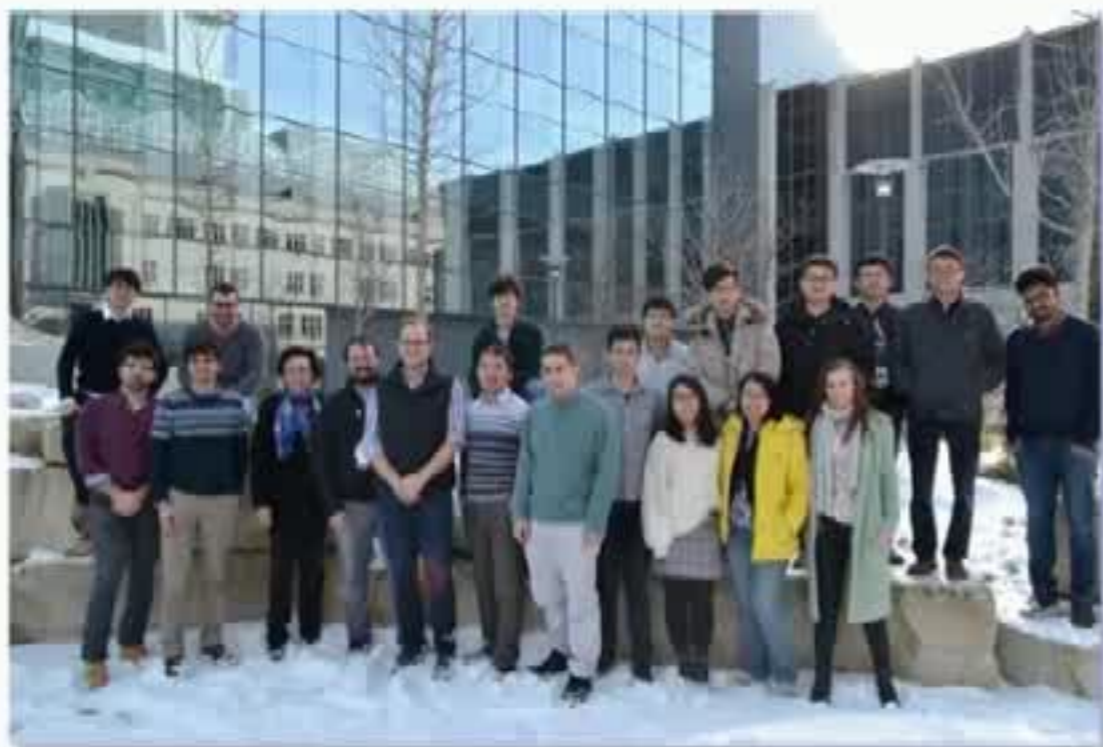


Towards D&D

Towards D&D

- Coupling of methods & coupling of software
 - Method development (theory & algorithms) is a critical need of the field
- Definition of automatic verification and validation procedures
- Integrated [theory-computation-data-experimental] strategies & automatic feedbacks

Acknowledgements



Qbox:
First-principles molecular
dynamics



WEST:
Many-body perturbation theory



SSAGES:
Reactive pathway identification
and free energy calculation



<http://miccom-center.org>

Collaborators: Dmitri Talapin (UoC), Stefan Wipperman (Max Planck, Dusseldorf), Francois Gygi (UCD), Juan de Pablo (UoC), David Awschalom (UoC), Francesco Paesani (UCD), T. Anh Pham (LLNL)